NAVAL POSTGRADUATE SCHOOL

MONTEREY, CALIFORNIA

THESIS

POWER MANAGEMENT SYSTEM DESIGN FOR SOLAR-POWERED UAS

by

Robert T. Fauci III

December 2015

Thesis Advisor: Alejandro Hernandez
Co-Advisor: Kevin Jones

THIS PAGE INTENTIONALLY LEFT BLANK

REPORT DOCUMENTATION PAGE			*Form Approved OMB No. 0704–0188*

1. AGENCY USE ONLY	**2. REPORT DATE** December 2015	**3. REPORT TYPE AND DATES COVERED** Master's thesis

4. TITLE AND SUBTITLE POWER MANAGEMENT SYSTEM DESIGN FOR SOLAR-POWERED UAS	**5. FUNDING NUMBERS**
6. AUTHOR(S) Robert T. Fauci III	
7. PERFORMING ORGANIZATION NAME(S) AND ADDRESS(ES) Naval Postgraduate School Monterey, CA 93943-5000	**8. PERFORMING ORGANIZATION REPORT NUMBER**
9. SPONSORING /MONITORING AGENCY NAME(S) AND ADDRESS(ES) N/A	**10. SPONSORING / MONITORING AGENCY REPORT NUMBER**

11. SUPPLEMENTARY NOTES The views expressed in this thesis are those of the author and do not reflect the official policy or position of the Department of Defense or the U.S. government. IRB Protocol number ____N/A____.

12a. DISTRIBUTION / AVAILABILITY STATEMENT Approved for public release; distribution is unlimited	**12b. DISTRIBUTION CODE**

13. ABSTRACT (maximum 200 words)

Drone technology has catapulted to the forefront of military and private sector research. Of particular interest are unmanned aerial systems that are able to stay airborne for extended periods by absorbing energy from the environment. This requires extreme aerodynamic efficiency in order to minimize the power required to maintain flight, and a recognition that every sub-system in this system of systems must operate at optimal levels in order to achieve this nearly perpetual flight. A critical component of a drone is the electrical hardware that optimizes solar energy absorption and manages energy storage. In particular, weight-to-power consumption demands consideration as inefficiencies quickly equate to additional power requirements. While off-the-shelf components are available for many of the individual pieces, none of these parts is optimized with size and weight in mind. Therefore, the impetus of this thesis is to examine the power management system within a systems engineering framework. This study includes maximum power point tracking, battery management, energy storage and flux tracking by the batteries, propulsion, avionics and payload components. The results drove the design and development of a compact single circuit that optimally integrates these sub-systems into a lightweight module for particular mission sets.

14. SUBJECT TERMS solar efficiency, maximum power point tracker, solar array, unmanned aerial system, power management	**15. NUMBER OF PAGES** 81
	16. PRICE CODE

17. SECURITY CLASSIFICATION OF REPORT	**18. SECURITY CLASSIFICATION OF THIS PAGE**	**19. SECURITY CLASSIFICATION OF ABSTRACT**	**20. LIMITATION OF ABSTRACT**
Unclassified	Unclassified	Unclassified	UU

NSN 7540–01-280-5500 Standard Form 298 (Rev. 2–89) Prescribed by ANSI Std. 239–18

THIS PAGE INTENTIONALLY LEFT BLANK

Approved for public release; distribution is unlimited

POWER MANAGEMENT SYSTEM DESIGN FOR SOLAR-POWERED UAS

Robert T. Fauci III
Lieutenant, United States Navy
B.S., Prairie View A&M University, 2007

Submitted in partial fulfillment of the
requirements for the degree of

MASTER OF SCIENCE IN SYSTEMS ENGINEERING

from the

NAVAL POSTGRADUATE SCHOOL
December 2015

Approved by: Dr. Alejandro Hernandez
Thesis Advisor

Dr. Kevin Jones
Co-Advisor

Dr. Ronald Giachetti
Chair, Department of Systems Engineering

THIS PAGE INTENTIONALLY LEFT BLANK

ABSTRACT

Drone technology has catapulted to the forefront of military and private sector research. Of particular interest are unmanned aerial systems that are able to stay airborne for extended periods by absorbing energy from the environment. This requires extreme aerodynamic efficiency in order to minimize the power required to maintain flight, and a recognition that every sub-system in this system of systems must operate at optimal levels in order to achieve this nearly perpetual flight. A critical component of a drone is the electrical hardware that optimizes solar energy absorption and manages energy storage. In particular, weight-to-power consumption demands consideration as inefficiencies quickly equate to additional power requirements. While off-the-shelf components are available for many of the individual pieces, none of these parts is optimized with size and weight in mind. Therefore, the impetus of this thesis is to examine the power management system within a systems engineering framework. This study includes maximum power point tracking, battery management, energy storage and flux tracking by the batteries, propulsion, avionics and payload components. The results drove the design and development of a compact single circuit that optimally integrates these sub-systems into a lightweight module for particular mission sets.

THIS PAGE INTENTIONALLY LEFT BLANK

TABLE OF CONTENTS

LIST OF FIGURES

LIST OF TABLES

THIS PAGE INTENTIONALLY LEFT BLANK

LIST OF ACRONYMS AND ABBREVIATIONS

A	ampere
ADC	analog-digital converter
COTS	commercial-off-the-shelf
DC	direct current
DMM	digital multi-meter
EEMS	Electrical Energy Management System
Hz	hertz
ISR	intelligence, surveillance, and reconnaissance
Li-po	lithium polymer
MPPT	maximum power point tracker
MSC	Military Sealift Command
NREL	National Renewable Energy Laboratory
PCB	printed circuit board
PV	photo-voltaic
PWM	pulse width modulation
SE	systems engineering
SoS	system of systems
TaLEUAS	Tactical Long Endurance Unmanned Aerial System
UAS	unmanned aerial system
USB	Universal Serial Bus
V_{DC}	volts, direct current

THIS PAGE INTENTIONALLY LEFT BLANK

EXECUTIVE SUMMARY

Solar-powered, extended-endurance unmanned aerial systems (UAS) are currently of great interest to researchers and especially military stakeholders. However, the amount of energy required to maintain truly continuous flight, coupled with the difficulty in obtaining that energy given current solar cell efficiencies, presents a daunting problem. This problem is made more difficult by the current state of battery technology.

A primarily solar-powered UAS such as the Tactical Long Endurance Unmanned Aerial System (TaLEUAS) attempts to solve that problem through the reliance on thermal lift throughout the day, mainly harvesting solar energy to charge the onboard batteries and only to power its control surfaces while searching for other thermals. In its current state, the onboard batteries are charged prior to flight and slowly discharged throughout the day, prompting a landing prior to sunset, as those batteries cannot be recharged due to a lack of a solar array (Camacho 2014).

The addition of a solar array would enable TaLEUAS to maintain fully charged batteries during the daytime, in preparation for the period of time that lacks sufficient solar irradiance to do so. At night, TaLEUAS would use its stored energy solely to maintain flight via its control surfaces and propulsion system.

The solar array laminated into TaLEUAS's wings does not currently produce enough voltage to charge a proposed parallel configuration of 4S3P li-po batteries. In order to accomplish this, a boost converter was implemented. Typically, a separate charge controller is also used to regulate the maximum voltage at the battery to protect it from an overcharged condition. However, by setting the boost converter's maximum output voltage to the proper level required by the battery, that function was accomplished internally by the MPPT module.

Initially, an equation was used to determine the proper resistance values to set the maximum voltage via voltage dividers on the input and output sides of the MPPT module. This equation was provided by the manufacturer. The resistance values found to be necessary were ordered and installed, but it appeared that the equation was not

sufficient for the amount of precision required in this case. A series of developmental tests were performed in the process of tuning the MPPT's maximum output voltage. Ultimately, three iterations of testing were required. Each required a change-out of resistors on the MPPT module, and in each iteration progress toward reaching the correct maximum voltage was made.

The Electrical Energy Management System (EEMS) developed by Camacho (2014) was initially used with a series of other commercially available components with lower operating capacities. These components included a lower capacity solar array, Genasun MPPT module, battery packs, and load to prove that the concept of an energy tracker/logger was viable.

During the devised operational test, the design herein used an adapted EEMS harness for use with the solar array mounted on TaLEUAS's wings, the smaller STMicroelectronics MPPT module, larger capacity li-po batteries, and the same 9.36 watt load used by Camacho. The EEMS provided its sensor readings to an Arduino Mega, which functioned as a datalogger.

The datalog was processed in MathWorks's MATLAB software to determine whether and where any electrical constraint was located within the system. By examining the graphs formed from the data, it was apparent that the charging system was adequate given the size of the load. A constraint was determined to exist in the energy storage (battery) components. While they may be the best choice available with regard to energy-density, and were suitable for providing power to a 9.36 watt load overnight, they are the weak point in the power system.

The use of the systems engineering (SE) process was ideal for solving this problem. There is a specified system level requirement, and a set of constraints, both of which are essential factors in SE. The requirement and any constraints on a possible solution were decomposed. After decomposition, these low-level solutions underwent developmental testing to solve problems at the lowest possible level, prior to integration. After integration, operational testing commenced in an effort to verify that the solution

was built correctly. Lastly, a successful operational test validated that the right solution was built for the problem.

REFERENCE

Camacho, Nahum. 2014. “Improving Operational Effectiveness of Tactical Long Endurance Unmanned Aerial Systems (TALEUAS) by Utilizing Solar Power.” Master’s thesis, Naval Postgraduate School.

THIS PAGE INTENTIONALLY LEFT BLANK

ACKNOWLEDGMENTS

My gratitude is extended to several people, but primarily, my thesis advisors, Dr. Kevin Jones and Dr. Alejandro Hernandez. Dr. Jones instilled in me the technical expertise and practical techniques when designing, building, and testing the system addressed in my thesis. Dr. Hernandez provided the stalwart leadership in ensuring that the project remained on schedule and budget. He was also instrumental in the development of this thesis as an actual systems engineering-specific topic.

I would also like to thank my parents for encouraging my curiosity, which allowed me to turn my hobby focuses into career endeavors. As a military child, science subjects were hard to turn away from when some of the world's greatest technology was employed by someone so close to me, my father. My father remains one of the greatest men I have ever had the pleasure of knowing. I will always admire what he has accomplished, and what he has pushed me to accomplish.

Of course, my wife deserves my gratitude as well. There were many long days and nights when academic projects kept me from coming home, and tolerating that time alone is no easy task. Luckily, the vast majority of the work occurred before news of the pregnancy. Our child will have big shoes to fill!

THIS PAGE INTENTIONALLY LEFT BLANK

I. INTRODUCTION

A. BACKGROUND

A problem exists within the United States Marine Corps regarding the amount of fuel consumed by its component forces. Fuel consumption has continued to rise with each new generation of hardware deployed to the field, and this consumption has increased at a rate greater than those systems that are designed to supply them with fuel. The risk is easily mitigated when operations are close to the shore, but as forces move inland, the risk to the fuel supply, and thus the force, increases. In addition, after forces have advanced to a position further away from the coast, the cost to supply fuel grows quickly, often requiring fuel to be flown to remote locations.

Most currently employed unmanned aerial systems (UAS) have inherent restrictions. All current long-endurance military UAS are powered by fossil fuels. For truly continuous operation, a transition to all-electric systems appears to be mandated by these restrictions. These limits include burning a finite amount of fuel, having to transit to and from a suitable airfield for maintenance, and most importantly, allowing limited in-theater loitering time. This amount of flight time significantly adds to the aircraft's fuel requirements and any reduced airtime limits the ability of the ground commanders to receive continuous surveillance. A form of renewable energy powered UAS is of great interest. It would decrease the fuel consumed by the force overall and simultaneously provide uninterrupted surveillance to commanders. Today, battery-operated UAS require the burning of fossil fuels to recharge batteries. Realization of this goal will decrease the reliance on fossil fuels transport and infrastructure and mitigate a portion of the operational risk to the force.

The Tactical Long Endurance Unmanned Aerial System (TaLEUAS) is a system of systems (SoS); it is a man-portable, powered glider that utilizes a combination of solar power and thermal lift to remain airborne, essentially indefinitely. In the prototype test aircraft, power is harvested by two strings of nine photo-voltaic (PV) cells which are connected in a series configuration. One string is laminated into each wing's structure.

This power is designated to be stored in an array of batteries in the aircraft's fuselage in a manner which will not interfere with the aircraft's flying ability.

The TaLEUAS airframe already exists. Likewise, the commercial-off-the-shelf (COTS) propulsion and avionics modules have also been designed and installed into the airframe. This places constraints on the design of the power management system. As a result, all derived requirements must be based off dimensional availability, theoretical cargo (weight) carrying capability, and power consumption requirements of already onboard components as well as those which may be installed in the future.

B. OBJECTIVES

The objective of this research is to design, build and test a power interface and management system for employment in the next-generation TaLEUAS airframe. The onboard subsystems require various voltage inputs and have various power requirements. Any proposed power system must account for those requirements. Two types of commercially available maximum power point trackers (MPPT) are considered, as well as battery architectures, and voltage regulation and protection circuits, which are typically seen in charge controllers. The power management system ultimately aims to increase the loiter time of TaLEUAS.

C. SCOPE AND ORGANIZATION

The scope and organization of this thesis is based on the systems engineering (SE) "vee" model. Each chapter relates to a particular portion of the model. Initially, a literature review is presented to familiarize the reader with research that has already occurred and to show where capability gaps have been found. These capability gaps form the very basis of the SE model.

A brief discussion on the practical use of MPPT circuits will enable the reader to understand the benefits of using an MPPT versus a pulse-width-modulated (PWM) charging circuit. A comparison and comprehension of the differences is important because the main interface between the PV array and the rest of the system will likely be one form of the two.

The power management system requirements derived from TaLEUAS's original concept of operations (CONOPS) are further defined through functional decomposition. From this decomposition, possible solutions are delineated. These solutions are compared against constraints with regard to dimensional, physical interface, and power output and consumption requirements. After the solution satisfies the constraints, the solution is then compared against the functional decomposition to ensure that every component actually contributes to the system.

We subsequently conducted a series of developmental tests, and made any modifications to COTS cards, or performed any connector installations, as required. The production work led into design verification after completion, notably through inspection of the components prior to the test. Later in any SE process, and in this research as well depending on the test results, validation takes place. Lastly, recommendations for future research are described based on any capability gaps found though the course of this research.

TaLEUAS has been successfully flown as a battery-assisted glider. However, without a method of in-flight recharging, it was restricted to daytime operations. The portability of the airframe gives the operator the option of launching the UAS by hand or with a small wheeled cradle if the terrain can support it. Onboard battery packs power the propulsion, computers, sensors, and avionics suites, which enable TaLEUAS to seek and navigate toward areas where thermal lift is in abundance. This thermal lift can come in the form of warm, rising air, as well as areas where differential pressure waves (wind) are strong enough to provide useful lift. Using a mathematical algorithm developed in previous work (Camacho 2012), the glider has reached altitudes of over 2700 feet. Reaching a higher altitude is possible but is dependent on geographic and weather conditions, according to Camacho (2012).

The latest generation of the already-existing airframe can be seen in Figure 1. An array of mono-crystalline silicon solar cells have been laminated into (and are an integrated part of) the airframe's left and right wings but have yet to function as a primary power source to subsequently provide energy for storage. Thus, the previously mentioned battery only powered TaLEUAS's onboard systems until its energy was depleted and the aircraft was forced to land.

Figure 1. Overhead view of TaLEUAS

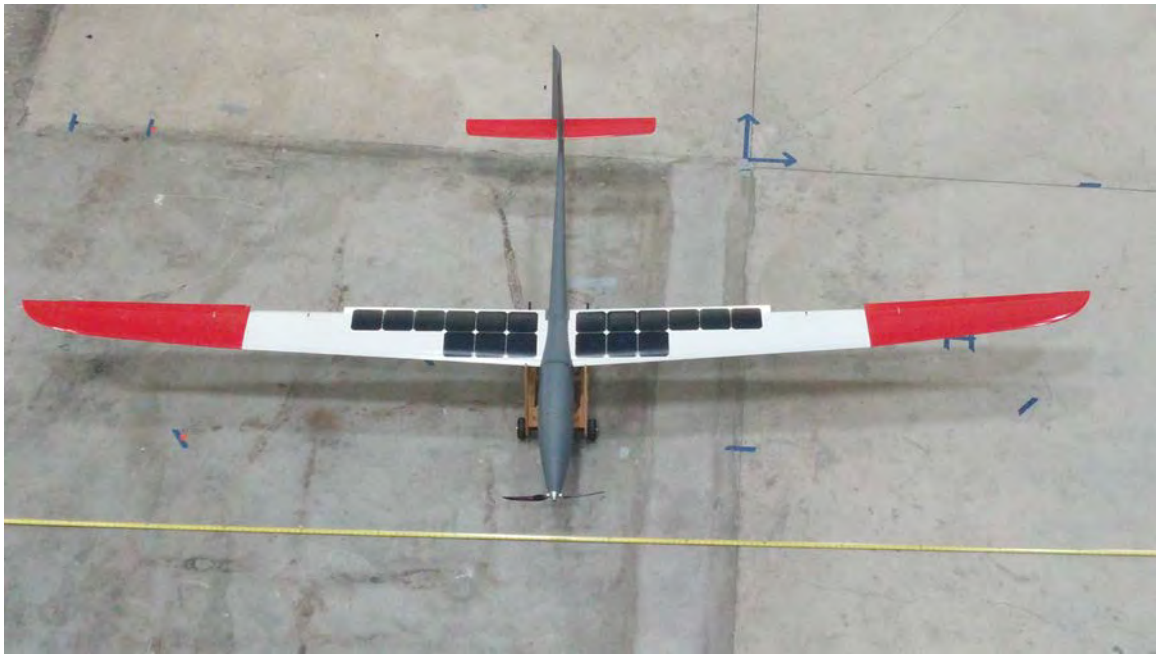

Ideally, swarms of these gliders can be used to provide around-the-clock surveillance with minimal human interaction after launch, but that is currently limited due to an insufficient balance and quantity of solar cells and batteries. Since these areas of thermal lift rapidly deteriorate after sunset, the glider must use its remaining power to navigate to a position of recoverability (i.e., it must land).

The primary benefit of this study is in enabling TaLEUAS to fly truly continuous missions or make significant progress toward that goal. However, other anticipated benefits are the determination of whether commercially available, lightweight MPPT modules are suitable, or can be made suitable for use aboard TaLEUAS given the current solar array configuration. Furthermore, the combination of an autonomous charging system and a modern lithium battery could prove to be unsuitable as well without proper over-charge protection.

Lastly, this research provides a method of reliably and efficiently regulating battery voltages to levels that are suitable for the onboard electronics to function.

II. LITERATURE REVIEW OF RELATED RESEARCH

A. MAXIMIZING SOLAR POWER CIRCUITS

The topic of integrating solar power into a UAS is of great interest to users with a stake in autonomous flight. Several relatively recent theses have focused on areas that will be discussed further in this study. A Naval Postgraduate School (NPS) thesis by Camacho (2014) focused on two major topics. One of those concerned the use of a commercially available MPPT circuit in a very similar manner to the research conducted herein. Earlier, an NPS thesis by Stephenson (2012) discussed the utilization of multiple MPPT circuits in parallel.

The primary advantage of coupling an MPPT with a PV array is to ensure that the maximum amount of energy is captured despite changing input conditions or output requirements (Stephenson 2012). This certainly holds true when developing design requirements for TaLEUAS, as input conditions constantly vary given the array's angle to the sun, and batteries' state of charge. Thus, the integration of an MPPT into TaLEUAS's charging system is crucial given the requirement for maximum power efficiency. Commercially available MPPT modules are sold with a wide variety of sizes, input and output power ratings, and onboard functionalities. Therefore, it is important to determine the unit with the proper combination of features that will meet the requirements for this specific application. As the design for the power management system is developed, these tradeoffs between features will be made.

In 2012, Stephenson attempted to use multiple MPPT modules in parallel to extract an optimum amount of power from a relatively small array. In an ideal situation, individual PV cells would have their own MPPT modules, which would enable two major advantages. The first can be considered more important to land-based solar systems; the optimization of the output power of each individual PV cell. This becomes essential when an array is installed in a manner in which individual cells have varying angles to the sun, or are partly shaded. The second advantage, which is more important to a primarily solar- powered aircraft, is the resilience provided by the use of parallel cells.

Figure 2. STMicroelectronics ISV009v1 MPPT/boost controller as-manufactured

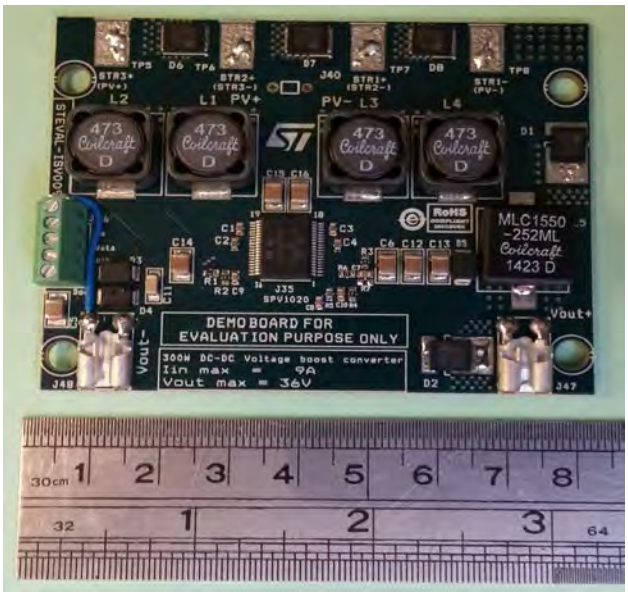

In Stephenson's thesis, the decision was made to abandon further research on an MPPT module which was manufactured by ST Microelectronics. This module is shown in Figure 2. The commercially available Genasun GV-Boost, shown in Figure 3, was used for his remaining research.

Figure 3. Genasun GV-Boost MPPT/boost controller as manufactured

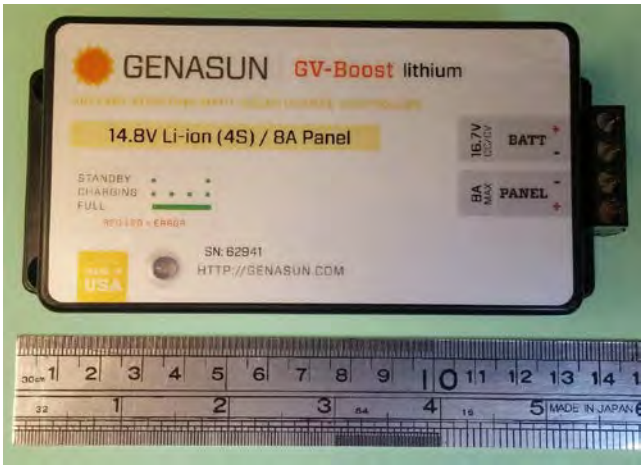

The STMicroelectronics board is advertised and sold as a demonstration tool to showcase the onboard SPV1020 processor, which contains the MPPT algorithm (STMicroelectronics 2011). The input and output voltages of the module are fixed at the factory. Changes to these voltages require modification of voltage dividers on the input and output sides of the board (STMicroelectronics, 2012). With the size of the onboard surface-mount-style components (0603 package) that require modification, human error in soldering can certainly become a problem source. The difficulty is only increased by the amount of copper present in the board.

After the modifications to voltage dividing resistors R1, R2, R3, and R4 were made to the STMicroelectronics board, instabilities were noted in the behavior of the card. Stephenson noted that after the required change in resistors, other pins on the embedded SPV1020 were not electronically connected to anything. Those unconnected pins led Stephenson to suggest that the build quality of the board was poor.

Another point of contention is with Stephenson's suggestion that the ISV009v1 and its onboard SPV1020 processor may not be designed to directly power a load. This can easily be resolved through the course of this research. Given the physical dimensions, size, and functionalities incorporated into the STMicroelectronics MPPT module, and the reliance on those features by TaLEUAS, more experimentation is warranted.

B. THE USE OF MULTIPLE MPPTS

Additionally, Stephenson (2012) demonstrated that the use of multiple MPPT circuits is beneficial when two panels experience drastic differences in irradiance levels. Given the construction of TaLEUAS's wings, and its relatively modest angle between them (five degrees), the wing mounted array will not experience drastic differences in irradiance levels. However, other benefits can be realized with the use of multiple MPPT circuits, most notably an increase in reliability through redundancy. In TaLEUAS's current configuration, the loss of function of a single cell in the 18-cell array will disrupt the entire supply of power to the battery, which would be considered a mission kill, and would require landing. However, multiple MPPT modules, if installed on each of the individual cells in the array, could ideally boost the individual PV cell's voltage to that

which is suitable for charging the battery. Each individual cell could theoretically then be installed in parallel with the others (or series, as required), which would allow the disruption of an individual cell's power output and not affect the remaining cells.

The use of multiple MPPTs, ideally one per PV cell, but realistically one per wing (nine cells) given the specifications provided by STMicroelectronics, may be worthy of further investigation. This involves a trade space which is outside of the scope of this thesis, however, as each wing is only capable of producing a maximum voltage of 5.58 volts. That voltage level is insufficient to even initialize an ISV009v1 module.

C. PREVIOUS SYSTEM-LEVEL WORK

In 2014, Camacho completed work which is fairly similar to this thesis as a proof of concept. An entire system from array to power consuming components was proposed and developed, and found to be feasible for further investigation (Camacho 2014). The system, as a proof of concept, did not focus on miniaturized components. Camacho developed a conceptual bus, named the Electrical Energy Management System (EEMS) to measure and determine power at each stage of management, to include the transfer of power from the array, through a Genasun MPPT module, to the power consuming and storage components. Camacho's EEMS block diagram is shown in Figure 4.

Figure 4. EEMS block diagram

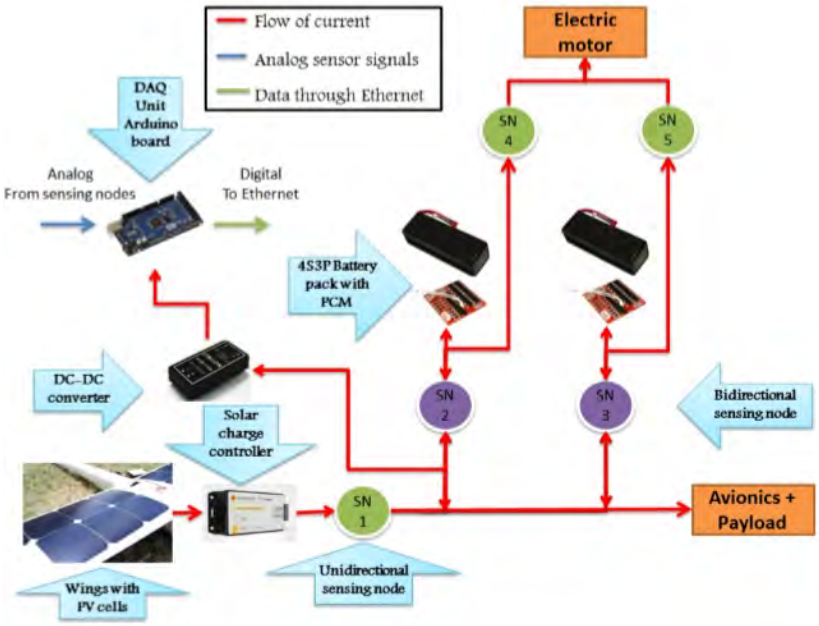

Source: Camacho, Nahum. 2014. "Improving Operational Effectiveness of Tactical Long Endurance Unmanned Aerial Systems (TALEUAS) by Utilizing Solar Power," 86. Master's thesis, Naval Postgraduate School.

The results from Camacho's (2014) test of the EEMS prototype noted that the peak power output of the PV array was 36 watts. From the graph provided in Figure 5 in that thesis, it is clear that over all, the system lacked the capacity to maintain uninterrupted power to the nine-watt load overnight. The point at which the batteries dropped the load is shown as the horizontal portions of the red, green, blue, and pink lines in Figure 5, and lasted approximately five hours each night. Additionally, the battery pack voltages only show a positive slope while the PV panel has a positive slope; this shows that the battery packs never reach a full charge prior to sunset.

In use onboard TaLEUAS, this situation would show that the configuration as previously prototyped is unsuitable and in need of significant improvement. The notion that the PV array only produced 36 watts at peak performance could signify that the weak point in the system was the array itself, as its predicted peak power output was approximately 50 watts based on the season. However, based on the EEMS block

diagram in Figure 4, the power output was actually measured at the output of the MPPT (SN1 in Figure 4).

Figure 5. Previous multiday experiment with the EEMS prototype

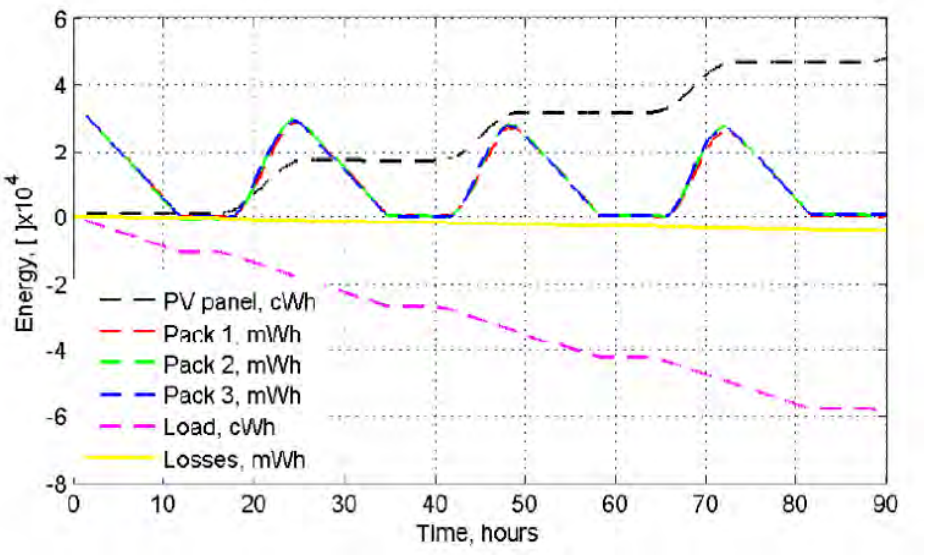

Source: Camacho, Nahum. 2014. "Improving Operational Effectiveness of Tactical Long Endurance Unmanned Aerial Systems (TALEUAS) by Utilizing Solar Power," 97. Master's thesis, Naval Postgraduate School.

Throughout the course of this research, we will attempt to use the EEMS harness, but it will likely require modification due to the change in end-user components. These changes will enable a feasibility determination of the monocrystalline-silicon PV array and smaller commercially available MPPT module, while still charging multiple 4S batteries in a 4S3P configuration. The use of the EEMS will also show the constraint in the electrical system, which will be determined to be one of three components (source, storage, consumption) through the manipulation of the load placed on it.

III. METHODOLOGY

A. INTRODUCTION

The methodology for this research follows the systems engineering "vee" model. Thus, the need for this technology is initially expressed, and functional requirements are derived from those needs. The design of the system is based on the stated functional requirements, and the ensuing tests determined whether or not those requirements were met.

B. REQUIREMENT IDENTIFICATION

The latest trend in military hardware appears that with each new generation of hardware comes an even greater thirst for fuel than the last. While this climbing fuel burn rate is certainly unfavorable in terms of efficiency, a more significant problem is the inability or constraints of providing fuel to those systems. Typically, fuel is transported into theater by Military Sealift Command (MSC) oilers, such as T-AO and T-AKE class ships. Upon arrival into theater, some form of friendly pier space is required to complete a mass-offload the fuel to airfield refueling systems, storage tanks or trucks.

When delivering fuel into hostile areas, the problem gets significantly worse. This often requires helicopter delivery of fuel via a robust bladder system at an extremely exorbitant cost and risk. A theme can be derived in that it currently requires excessive fuel to move fuel. This all leads to increased operational risk: the risk that forces will deplete their resources before resupply, and risk of enemy combatants will interrupt the flow of fuel to a friendly force at any of a number of strategic chokepoints.

One family of fuel-consuming weapons or surveillance systems, which consistently operates over hostile areas, is the UAS. Thus, it is fitting that the overarching capability gap that will be discussed in this thesis is the inability to reduce the use of excessive amounts of time and fuel in support of surveillance on the battlefield. This is an increasingly important mission for the UAS family of systems. Systems currently in use, such as the MQ-9 Reaper and others, are required to transit to and from the area that is surveilled, which requires time and fuel. These systems-of-systems also require pilots,

which while not onboard, are still subject to typical human factors design requirements in the building of operating consoles, fatigue analyses, and eventual human error. A method of conducting continuous aerial surveillance without further burdening the fuel supply infrastructure does not currently exist, and the desire for such a system has been expressed.

C. REQUIREMENTS ANALYSIS

The thesis by Camacho (2014) demonstrated the ability of truly autonomous aircraft to constructively interact with each other. When taking this concept into consideration, it becomes evident that a broad mission such as battlefield surveillance can be split among a number of assigned autonomous systems. Decomposed even further, the amount of energy required to complete that mission can be split among multiple systems (Camacho 2014). This division of required energy is of utmost importance when considering an option which relies on solar irradiance because of the difficulty in obtaining it.

Interaction in flight can help mitigate the relatively low efficiency of the installed mono-crystalline silicon photo-voltaic cells (currently 22.5%, but 24% are available), as well as the current energy storage capacity when utilizing Lithium-Polymer battery packs. A single UAS relying on this energy production and storage technology would likely prove unsuitable. However, if multiple systems were able to carry the load of conducting portions of a given surveillance mission at different times, thus splitting the total energy requirement among multiple nodes as needed, a feasible solution becomes much easier to obtain. Converting this solar energy, as well as storing and providing it to onboard devices will require consideration of the following constraints. These constraints translate into system-level requirements and are further decomposed into sub-system requirements.

1. Physical Dimensions

As stated previously, a major constraint placed on the problem is that the TaLEUAS airframe already exists. As seen in Figure 6, the available space is fairly limited. At the most spacious portion, it measures only 4.5 inches wide and 6.5 inches

tall. This certainly restricts the number of available solutions when considering energy storage. All proposed electrical components, and the boards on which they reside, must be compact enough to be integrated into this available space. Proper routing of wires or cables is also required to protect against accidental short-circuits which could lead to a loss of control, or fire in the worst of cases. If an interface is required with other sub-systems, that interface must be designed into the proposed solution.

Figure 6. TaLEUAS fuselage transverse dimension

2. Weight

The constraint placed on the weight of any individual component is doubly important when considering it for use on an aircraft. TaLEUAS's wings not only require the ability to create a sufficient amount of lift to carry the onboard sensors, computers, and other equipment, but each individual component must be carefully placed in order not to interfere with the in-flight stability of the aircraft. Any in-flight instability will increase the energy consumed in correcting that error by the control surfaces or autopilot. Likewise, every individual component's weight must be minimized to the greatest extent possible because any energy expended in keeping excess weight airborne equates to

additional energy storage requirements. This ultimately contributes to the overall energy efficiency of the system.

3. Power Consumption

Considering this research topic, perhaps the most important of the constraints mentioned is the amount of power consumed by each sub-system onboard. The previous generation of TaLEUAS used a multitude of electronics, to include an autopilot unit with controls, computer, among other avionics. This load alone represents an approximate load of 18 watts by inspection. However, an assumption that updated commercial systems can reduce the power consumption to nine watts, with the exception of the propulsion system, is reasonable. Therefore, the simulated load during any testing will continuously consume nine watts.

4. Power Production

As mentioned previously, the 18 individual cells in the PV array laminated into the wings are nominally capable of providing .62 V_{DC} each and have previously been assembled into a series configuration. When exposed to full sunlight, the panel has an output voltage of 11.2 V_{DC} (open-circuit voltage), and is capable of providing six amperes of current (short circuit). This voltage level is not sufficient to fully charge the installed battery packs without some form of transformation or boosting. Therefore, the solution must be capable of raising DC voltage levels.

Of primary concern are the battery packs. The 4S lithium-poly packs proposed to be used on TaLEUAS have their own set of constraints, with a maximum charging voltage of 16.82 V_{DC}. Overcharging this variation of battery typically results in a spectacular fire.

The proposed solution must be capable of providing power to all of the onboard electronics. While this seems fairly straightforward, the electronics used require various levels of voltage. Thus, the solution must be capable of regulating voltages at varying levels.

Lastly, charging the batteries with either a traditional pulse-width-modulating (PWM) or an MPPT device will have a significant impact on the efficiency of the power production system. PWM chargers are typically larger, and have lower efficiency ratings, which were reasons that MPPT devices were developed. The importance of the use of an MPPT charger is not so much in the additional power gained, but in the power that isn't lost to heat. When considering power input and output, the proposed solution must maximize efficiency.

D. DEVELOPMENTAL TESTING

All developmental testing occurred with the goal of meeting the specification requirements that have been laid out. Developmental testing does not give a complete or even accurate picture of the whole-system's operational performance (Stevens 1979, 9). Independent verification that individual components operate as desired can improve the probability of successful operation when those components are combined to operate as part of a system. Though successful operational testing is not guaranteed by successful developmental testing, this form of testing is absolutely vital in the progression towards operational testing. The detailed design accomplished in this chapter is usually associated with the "vee," on the lower left side of the model.

Proper utilization of the STMicroelectronics ISV009v1 MPPT board required skillful modification of four voltage dividing resistors on both the input and output sides of the onboard SPV1020 chip. This was realized through reviewing documentation provided by STMicroelectronics, and subsequently verified during the review of applicable literature. After determination of the proper resistance values per Equations 1 and 2, open-circuit voltage readings were taken from the output of the board to determine if the desired effect was achieved (Ragonese and Ragusa 2012).

$$\frac{R1}{R2} = \frac{V_{OC}}{1.25} - 1 \qquad (1)$$

R1 and R2 represent the resistors used to partition the input voltage, and this input voltage must be scaled to the reference voltage (1.25 V_{DC}) of the Analog-Digital

Converter (ADC) integrated in the SPV1020. V_{OC} represents the open-circuit voltage of the PV panel (Ragonese and Ragusa 2012, 32).

The output side of the MPPT board uses a similar method to partition the output voltage; by way of a voltage divider circuit. Equation 2 determines the maximum output voltage:

$$\frac{R3}{R4} = \frac{V_{out\_max}}{1.00} - 1 \qquad (2)$$

R3 and R4 represent the two resistors used to partition the output voltage. V_{out_max} represents the maximum output voltage at the load (Ragonese and Ragusa 2012, 34).

Direct current voltage which emulates the power provided by the PV panel was provided to the ISV009v1 by a Protek 3015 DC power supply, and the MPPT's open-circuit output voltage was then read by a Fluke model 115 digital multi-meter (DMM). The use of a benchtop power supply enabled indoor testing but this model was limited to 1.5A of current. For all purposes other than a very simple test of the MPPT card, this represented a significant problem. When the power supply was in operation at the correct voltage of $11.2V_{DC}$, the maximum power output is approximately 25% (~16W) of what would be expected in realistic conditions, which is near 60W. When the load required current in excess of 1.5A, the power supply enters a self-protection mode, and this limits the current at 1.5A.

The cessation of charging at the correct output voltage is essential, as the MPPT is also being used as a charge controller. One alternative method of providing the correct voltage to the battery bank would be to configure the MPPT input & output voltage dividers mentioned above to boost the voltage above $16.7V_{DC}$, and regulate it at $16.7V_{DC}$. This would require external voltage regulators to perform that function, which are not readily available, add weight, and waste energy in the form of heat. Given the importance of the cessation of charging at the proper level, multiple iterations of testing were required, as tolerances of resistors varied. To combat this variance, high precision resistors were used, all with a tolerance of .1%. After the initial bench tests proved that

the ISV009v1 as modified could provide a suitable voltage level, further testing commenced.

The next developmental test will prove to be a series as expected. We first integrated the ISV009v1 with TaLEUAS's actual PV array and a single li-po battery pack. This test determined whether the ISV009v1 module was suitable for charging a battery by way of boosting the input voltage as designed, and decreasing its output current as the input voltage approached the reference voltage to prevent overcharging. The testing occurred outdoors in full sunlight. Data (voltage and current over time) was logged digitally via an Eagle Tree eLogger V4, which has a 50 Hz sampling rate capability (Eagle Tree Systems 2015). Simultaneously, an Eagle Tree Power Panel displayed the conditions to ensure that voltages and currents remain at safe levels, and could be disconnected if a problem arose. Both of these devices are shown in Figure 7 (Eagle Tree Systems 2013).

Figure 7. Eagle Tree Systems eLogger V4 and Power Panel devices

Source: Eagle Tree Systems. 2013. "Elogger v4." Accessed July 2, 2015. http://www.eagletreesystems.com/index.php?route=product/product&path=62&product_id=54.

Upon the satisfactory demonstration of the ISV009v1's charge controlling functionality, further testing was performed in a similar manner with an increased battery bank capacity. Each increase in capacity will showed that the ISV009v1 is capable of operating for an extended amount of time.

E. OPERATIONAL TESTING

Operational testing attempts to determine the performance of a system under the most current operational conditions (Stevens 1979, 4–5). The process described by Stevens has four principal objectives which he lists as:

1. To determine whether a system, in combination with its operators, maintenance personnel, and supporting equipment, can fulfill its current missions and objectives.

2. To develop methods and procedures for the optimum employment of new systems or for the use of old systems in new ways to satisfy new missions and objectives or to interface properly with new equipment

3. To establish the limitations, characteristics, and capabilities of a new system to determine how it can best be integrated into an entire management structure and what personnel and logistic requirements exist for the proper support of the system.

4. To provide information that will assist in the research and development of new systems through documenting needs for improved performance or different performance and in determining the deficiencies from a performance standpoint of the system under test.

Though time was unavailable to support true operational testing of the TaLEUAS system as a whole, an operational test of the power management system was fully feasible. Information such as reliability, availability, and maintainability data can be obtained by completing extended tests of this system, but is not in the scope of this thesis.

Starting the operational test process involves the development of critical issues. Critical issues can be expressed in the form of questions about a system that reflects uncertainties about its effectiveness (Stevens 1979). Concerning this operational test, the following items have been identified as critical issues:

- Can the power management system maintain power to the onboard systems overnight?
- Can li-po batteries be charged safely aboard a UAS?
- Can the system support running a load and simultaneously charging a battery?
- Can the system be installed into the TaLEUAS airframe?

The operational test that was conducted used the EEMS harness referenced in Figure 4. The wing-mounted array was connected to the ISV009v1 and battery packs via the harness. The EEMS was modified to interface with three 4S li-po battery packs in a 4S3P configuration, as well as a 12V (step-down) switching voltage regulator which provided power to a simulated load. A transient period was forced into the system via unequally charged batteries to determine whether the system was capable of responding adequately and transitioning into a steady state. The unidirectional and bidirectional current sensors installed in the EEMS harness enabled the tracking of energy across six analog inputs, which was logged by an Arduino Mega 2560 with the help of a data-logging shield and secure digital (SD) memory card.

The load included in the operational test is an important part of this extended duration experiment. Most importantly, the proposed nominal load of 9.36 watts induced by the fan bank constitutes approximately half of the steady-state load posed by the current onboard electronics suite. This onboard electronics suite load is considered steady state because it remains in constant operation. Given currently available technology, this simulated load can be considered a reasonable parametric estimation after later upgrades are made to TaLEUAS. This operational test proved whether or not the proposed power management system is capable of powering the load continuously. If so, there may be excess power to provide a safety factor for days with less than ideal solar irradiance, or additional loading could be accommodated. If not, the load will require adjustments.

The test rig was constructed in a weather resistant enclosure. This plastic case contained all of the equipment with the exception of the solar array, which was fully exposed to the ambient environmental conditions. The testing location chosen was the highest working level at Spanagel Hall, at the Naval Postgraduate School, Monterey, California.

F. ANALYSIS OF TEST RESULTS

Upon completion of the week-long operational test, the test rig was removed from Spanagel Hall’s roof, and the SD memory card was extracted from the Arduino data-logger. The raw data from the memory card was subsequently imported into MATLAB

and scaled into relevant measurements. These measurements showed the total power from the ISV009v1 during the day and likewise each battery pack at night, as well as how that power was continuously distributed throughout the testing period. Major points of interest were the regulation of bus voltage at charge completion, as well as the determination of excess capacity in charging or storage, or lack thereof. These results indicated where the electronic constraint was and if any necessary changes in the number or PV cells, load capacity, as well as energy storage capacity existed.

IV. DATA ANALYSIS

A. DEVICE CHARACTERISTICS

We will begin the analysis by comparing the physical characteristics of the STMicroelectronics ISV009V1 and Genasun GV-Boost MPPT modules. The most obvious difference is in the appearance and layout; the STMicroelectronics board subjectively looks very crude, operator-unfriendly, and is completely unshielded from adverse environmental conditions. The Genasun module has been designed into a plastic enclosure, has a flashing LED light to indicate to the operator when the battery is fully-charged, and has aesthetically pleasing labelling. Both units provide mounting holes; the difference is in the location of them. The STMicroelectronics module's mounting holes are placed directly in the printed circuit board (PCB), while the Genasun unit's are provided on its plastic case.

Another major difference between the units lies in the physical interfaces. The Genasun once again uses more operator-friendly screw-clamps to secure the input and output wiring, while the STMicroelectronics unit relies on solder pads on the input side, and female blade connectors on the output side. The solder pads and blade receptacles used on the STMicroelectronics module require additional skill in soldering, while the Genasun unit requires a simple wire stripping procedure to connect the PV array as well as the rest of the system.

The weight difference between the two units is significant. When the enclosure is removed from the Genasun unit, the reason why is clear. The toroidal inductor which is presumably used in the voltage boost process is the bulk of the Genasun unit's weight. The STMicroelectronics module uses four much smaller inductors to accomplish the same goal. The Genasun module weighs 179 grams, while the STMicroelectronics module weighs 46 grams. Both modules were weighed as manufactured, with no modifications made. It is important to note that the STMicroelectronics unit does not have an enclosure, and it is likely that the Genasun would never be used with its enclosure. Removing the Genasun enclosure brings the unit's weight to 100g. The TaLEUAS's fuselage access panels are not yet weather-tight, but the prototype is not

operated in foul weather, so removing the enclosure or selecting a unit without an enclosure is not a problem at this time.

As the STMicroelectronics board is significantly lighter, it is also significantly smaller. The Genasun module measures 14x6.5x3.1cm, which is approximately 40 percent larger than the STMicroelectronics module's 8.1x5.4x1.5cm measurement. This reduction in size allows for greater flexibility in location. This is useful because TaLEUAS's fuselage is already crowded with other electronics suites. It will also aide in the optimal amount and routing of wiring, which is another source of weight. STMicroelectronics manufactures even more compact demonstration boards, however, which may reduce weight even further. For example, the STMicroelectronics ISV008v1 demonstration board can be modified to weigh only 25 grams with its smaller board (75mm x 27mm), and still handle up to 100 watts.

Given that TaLEUAS is not designed to be maintained by operators, and that aesthetics are not a factor in the decision-making process, the above comparison of the physical characteristics lead to a decision to pursue the development of the STMicroelectronics MPPT module.

B. DEVELOPMENTAL TESTING RESULTS

Developmental testing is necessary to ensure that individual components are correctly configured prior to the commencement of operational testing, and is typically found at the middle of the systems engineering "vee" model.

1. Developmental Test 1

The initial test confirmed that the ISV009v1 functioned as designed and manufactured. Using the Protek 3015 power supply, 11.2 V_{DC} was applied to the input of the ISV009v1. The output was indeed boosted to 24 V_{DC}; therefore, the MPPT card performs as designed.

With that confirmed, initial modifications were made to the module in an attempt to change the output voltage. Using Equation 1, the decision was made to replace R1 and R2 with 505K and 63.4K ohm resistors, respectively. Likewise, using Equation 2, R3 and R4 were replaced with 1M and 68K ohm resistors, respectively. Once again, the module was then connected to the DC power supply and 11.2 V_{DC} was provided to the input. The

Fluke digital multi-meter then measured the V_{OC} as $17.3V_{DC}$. Although this voltage was measured above the $16.7V_{DC}$ required to charge the battery, that voltage was expected to drop when a load was applied.

The next step in verifying that the MPPT performed as desired was to setup a test with some of the components that would be used onboard TaLEUAS. As was previously described, the actual TaLEUAS wings in addition to one of the actual batteries were gathered and assembled into the configuration seen in Figure 8.

Figure 8. Developmental test configuration for iterations 1&2

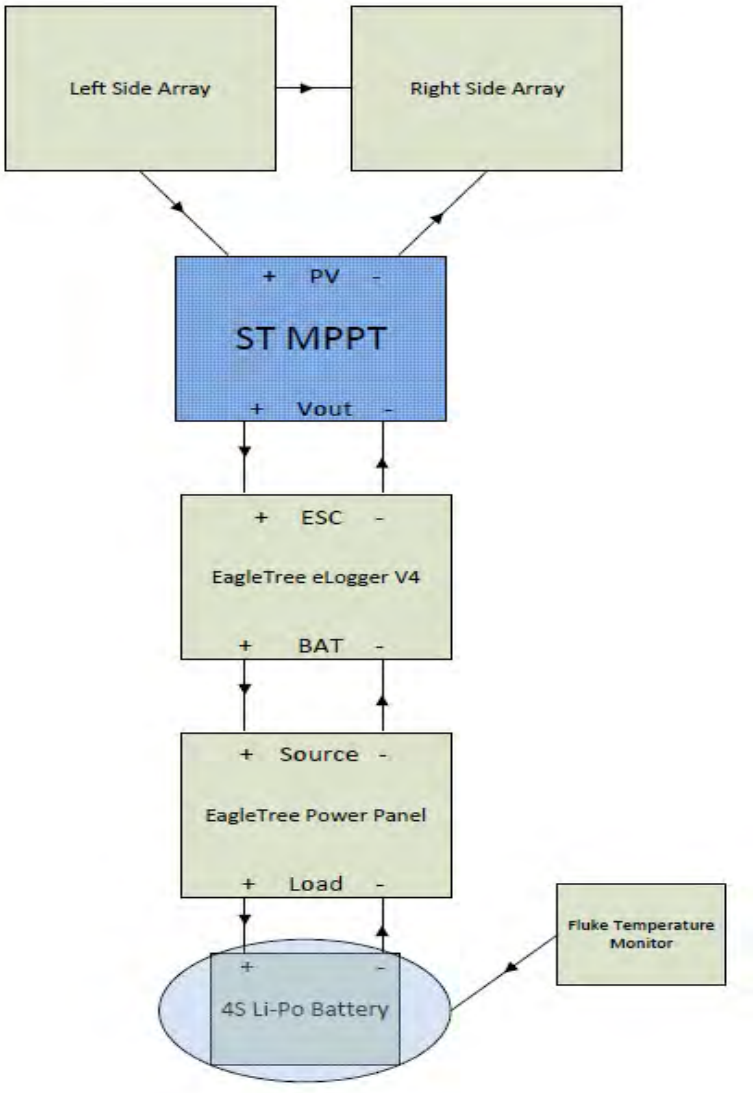

Using the Eagle Tree e-Logger on June 18, 2015, the graph in Figure 9 was obtained. The li-po battery received the charge as expected; however, the MPPT stopped charging prior to reaching the correct voltage. The pack voltage is seen in the graph as the blue line and power in watts as the orange line. The blue line plateaus at 16.44 V_{DC}, which is .26 V_{DC} short of a "full" indication. However, when the blue line's plateau was approached, a steep drop-off was observed in the power (orange) indication. This shows that the MPPT is ceasing the charging process effectively, but an adjustment was needed to increase the point at which charging is stopped. That adjustment was made to R3 and R4 for the second iteration, while R1 and R2 remained the same. The steep variations in the orange line were caused by partial cloud cover that day and were expected.

One interesting fact to note in Figure 9 is the peak power output. Even on this first developmental test, a peak power output of 50.94 watts was achieved. This is a significant increase from the peak power output of 36 watts reported in the previous thesis while using the Genasun MPPT (Camacho 2014).

The graph correlated to what was observed via the Eagle Tree Power Panel. Care was taken to ensure that the battery pack voltage never exceeded 16.7V_{DC}, which was accomplished by having the entire test monitored in person. The Power Panel allowed the monitoring of real-time voltages, power, current, and cumulative current. The PV panel allowed for a quick disconnection if levels approached or exceeded what is considered safe. In addition to the safety measure provided by the power panel, a separate Fluke multi-meter with an integrated temperature monitor allowed confirmation that the battery temperature did not exceed a safe level, which we considered 20 ^{o}F higher than ambient, which ranged between 60 and 62 ^{o}F from 1130L to 1203L. After the test, the battery was brought to a maintenance station and discharged to 50 percent of capacity (15.3V_{DC}) for safe storage in accordance with the Naval Postgraduate School's Safety and Usage Procedures for Lithium Polymer Batteries.

Figure 9. Developmental Test 1 – Initial MPPT test with single 4S li-po battery

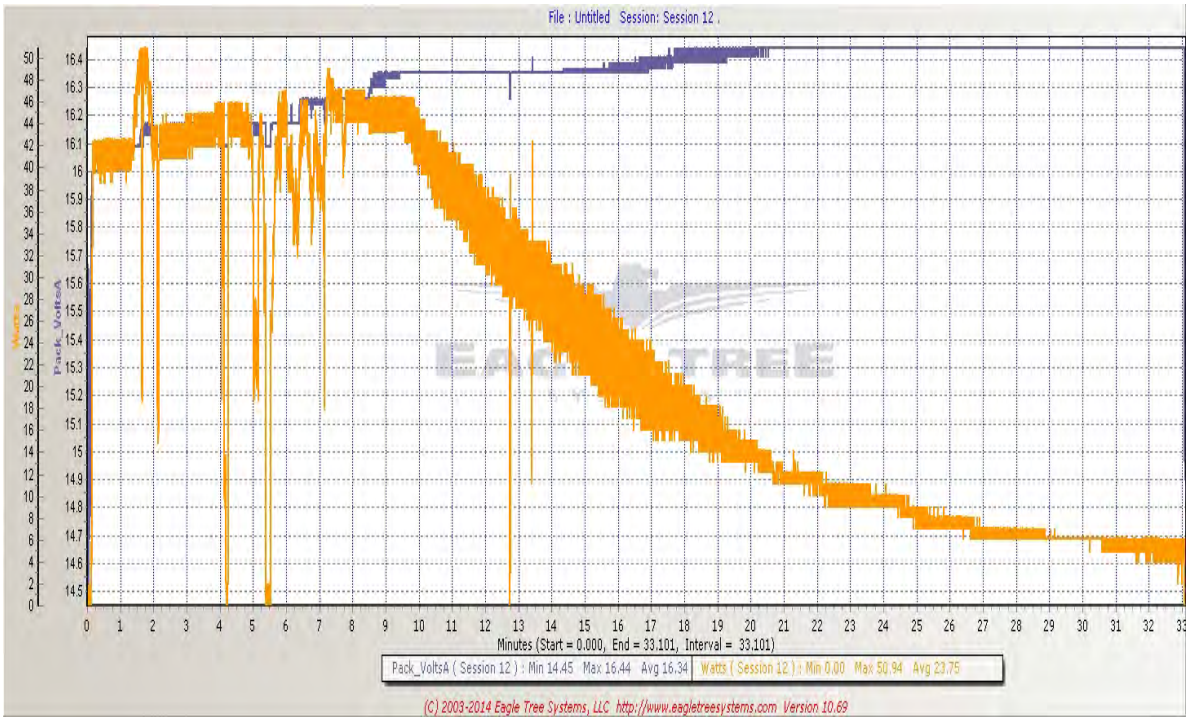

2. Developmental Test 2

As mentioned previously, the second iteration did not involve any changes to the input side of the MPPT module. On the output side however, in order to increase the output voltage, the resistor in the denominator's place of Equation 2 (R4) was decreased to the next smallest size on hand, which was a 63.4K ohm resistor.

Figure 10 shows the graphed data-log from the test which was completed on July 6, 2015. Pack voltage is again represented by the blue line; power is represented by the orange line. Current was monitored on this log for convenience and is shown as the red line. Once again the peak power output exceeded expectations and momentarily reached 56.35 watts. That level of solar irradiance was not maintained throughout the 6 of July, however. The graph also indicates that the peak battery voltage was monitored as reaching 16.96 V_{DC}; however, that reading was faulty and occurred when the battery was disconnected and reconnected in order to check the battery voltage with a digital multi-meter. The multi-meter was used as a source of verification because the MPPT was still

charging when the Eagle Tree Power Panel displayed a voltage of 16.7V_{DC}. As was performed in the first developmental test, the battery temperature was continuously monitored, and was never found to be a problem.

The results from the second test did provide some other important information, however. First, the MPPT proved that it could perform its job for a significantly longer period of time than was previously displayed. Second, changing only the R4 resistor verified that the output voltage can be altered with relatively minor modifications. Most importantly, the necessary resistor was found to be between 63.4K ohms and 68K ohms.

Figure 10. Developmental Test 2 – MPPT test after further modifications to output voltage divider circuit

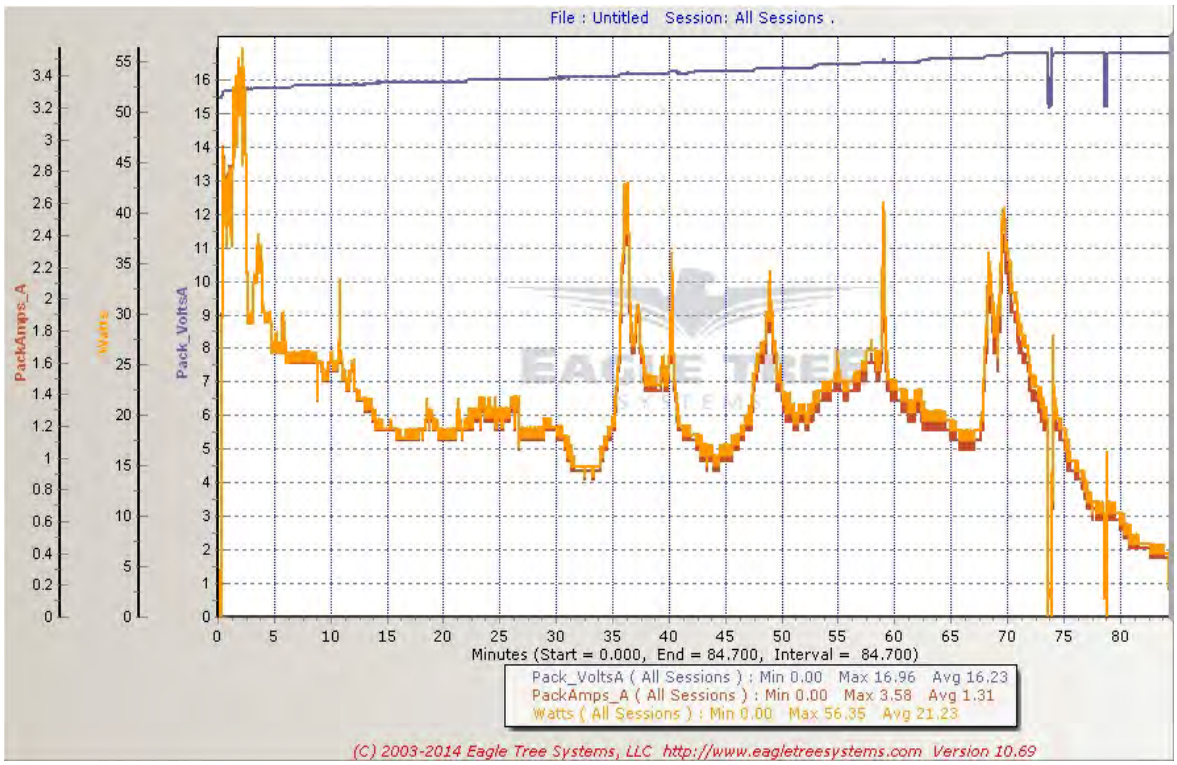

The only resistor found to be readily available in the correct size, tolerance, and power rating, was a 66.5K ohm component. It was subsequently ordered from Digi-Key. The 63.4K ohm component was then de-soldered and removed, and the 66.5K ohm component soldered into its place.

3. Developmental Test 3

After the installation of the latest resistor, another attempt to zero-in on the correct maximum output voltage occurred. On July 9, 2015, the setup in Figure 7 was once again assembled with a minor modification. The entire system was assembled as seen in Figure 11.

Figure 11. Developmental test configuration for iteration 3

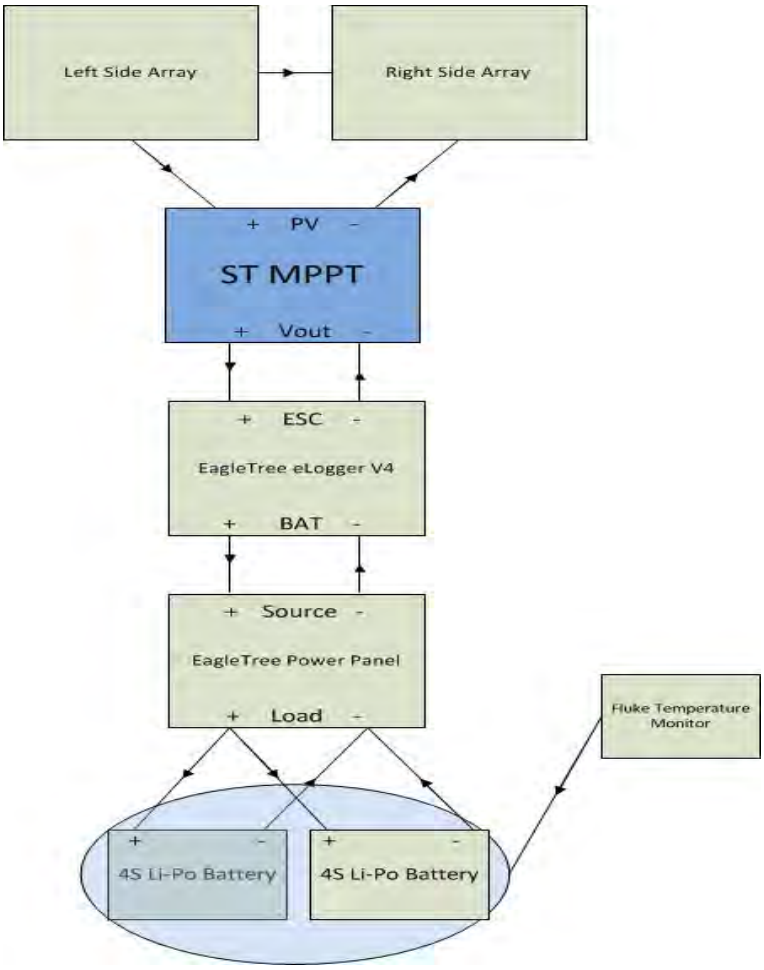

The third developmental test iteration, for which the graph is shown in Figure 12, shows that the MPPT ceased charging at a voltage of 16.68 V_{DC}, which was also verified with a Fluke digital multi-meter at the conclusion of the test. Based on the availability of suitable components, this is seen as an acceptable and optimal voltage. The cessation of charging is shown as the steep decline in the red and orange lines (current and power,

respectively) as the blue line (voltage) approached the plateau at 16.68V_{DC}. As occurred in the other two iterations, peak power output again exceeded 50 watts. The test lasted almost three hours, and shows that the MPPT is suitable for testing with an even higher level of realism and duration. A method of data-logging multiple inputs for an extended period of time is required.

Figure 12. Developmental Test 3 – Final modification to MPPT and addition of a second 4S li-po battery pack

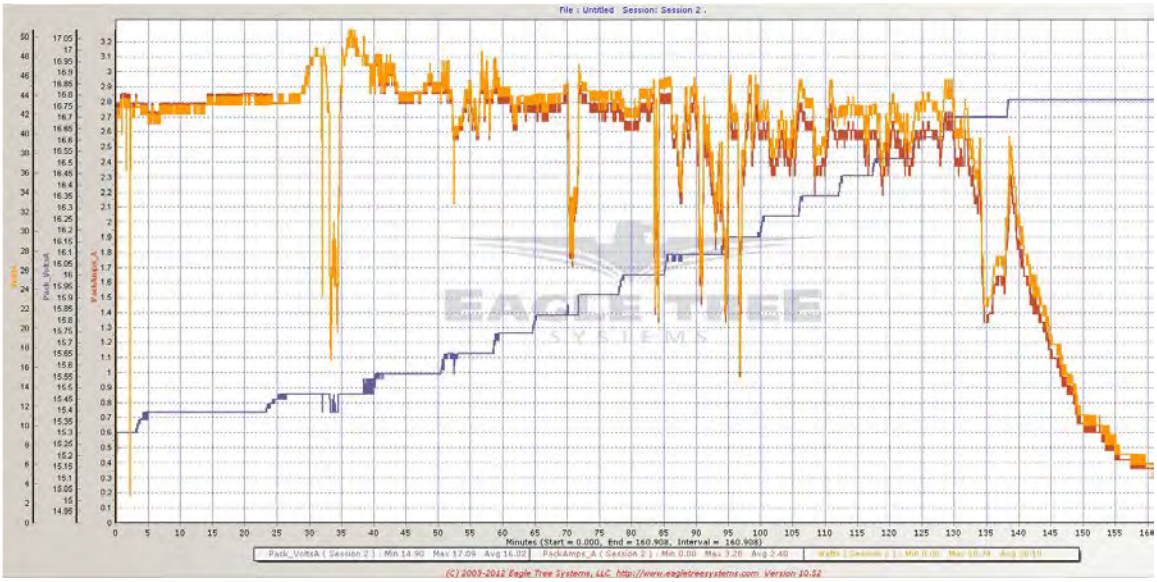

C. ARDUINO-BASED DATALOGGER DEVELOPMENT

During the course of making preparations for the operational test, another requirement was derived. Considering the complexity of the EEMS harness, and the multiple sensors installed in it, the Eagle Tree Systems eLogger v4 is not suitable for operational testing as it only logs a single input. The proposed data logging system has to be capable of logging seven analog inputs for a period of seven days, must be externally powered, and must be capable of providing power to the EEMS sensors. These requirements are based on the proposed test length, existing EEMS harness specifications. The Arduino Mega 2560 microcontroller was chosen to meet this requirement. This is because the unit itself and the Ethernet Shield used to store the data-logs were already on hand in the laboratory.

The Ethernet Shield was chosen because it enables onboard SD data logging functionality. This specific functionality enabled the Arduino to act as a standalone logging system. Additionally, the software to operate these devices is open source and already written. The specifications for the microcontroller are displayed in Figure 13.

Figure 13. Arduino Mega 2560 technical specifications

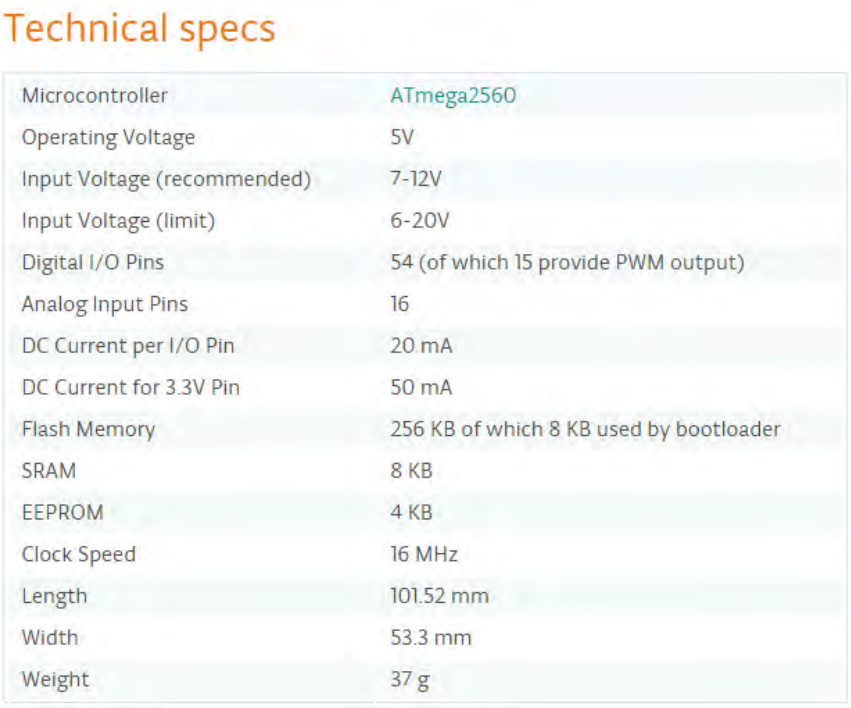

Technical specs

Microcontroller	ATmega2560
Operating Voltage	5V
Input Voltage (recommended)	7-12V
Input Voltage (limit)	6-20V
Digital I/O Pins	54 (of which 15 provide PWM output)
Analog Input Pins	16
DC Current per I/O Pin	20 mA
DC Current for 3.3V Pin	50 mA
Flash Memory	256 KB of which 8 KB used by bootloader
SRAM	8 KB
EEPROM	4 KB
Clock Speed	16 MHz
Length	101.52 mm
Width	53.3 mm
Weight	37 g

Source: Arduino. 2015. "Arduino Mega 2560 Overview." Accessed August 24. https://www.arduino.cc/en/Main/ArduinoBoardMega2560.

The microcontroller itself is not suitable for storing the data from the inputs, only processing it. Luckily, the Arduino family of microcontrollers is supported by a large online community of enthusiasts as well as by private companies. Many types of "shields" have been developed which are quickly installed onto the Arduino to serve specific purposes. The one that is discussed here is the Ethernet Shield.

A specific code is required to operate the Arduino and its shield as desired. This basic code is freely provided and is actually an inherently available part of the Arduino compiling program after installation on a personal computer. The code required minor

additions in order for it to serve our purposes, mainly to add in a timestamp at each recorded event. This timestamp is necessary because it allows certainty of the analysis of the PV system's behavior throughout the day. The code was then compiled and transferred onto the Arduino. The code continuously runs as long as power is provided to the unit. It is attached as Appendix A.

In order to test the functionality of the Arduino and Ethernet Shield setup, we conducted a short bench test. The EEMS harness's seven pins were connected to the microcontroller's analog inputs, seen in Figure 14. Power was provided to the microcontroller via a laptop computer's USB interface for convenience because the test results were being monitored simultaneously on the laptop. Power may optionally be provided from 120VAC via an AC-DC adapter; in fact, this will likely be required when performing the operational test due to the isolation from other computers.

Figure 14. Arduino Mega 2560 with Ethernet Shield installed and connected to EEMS

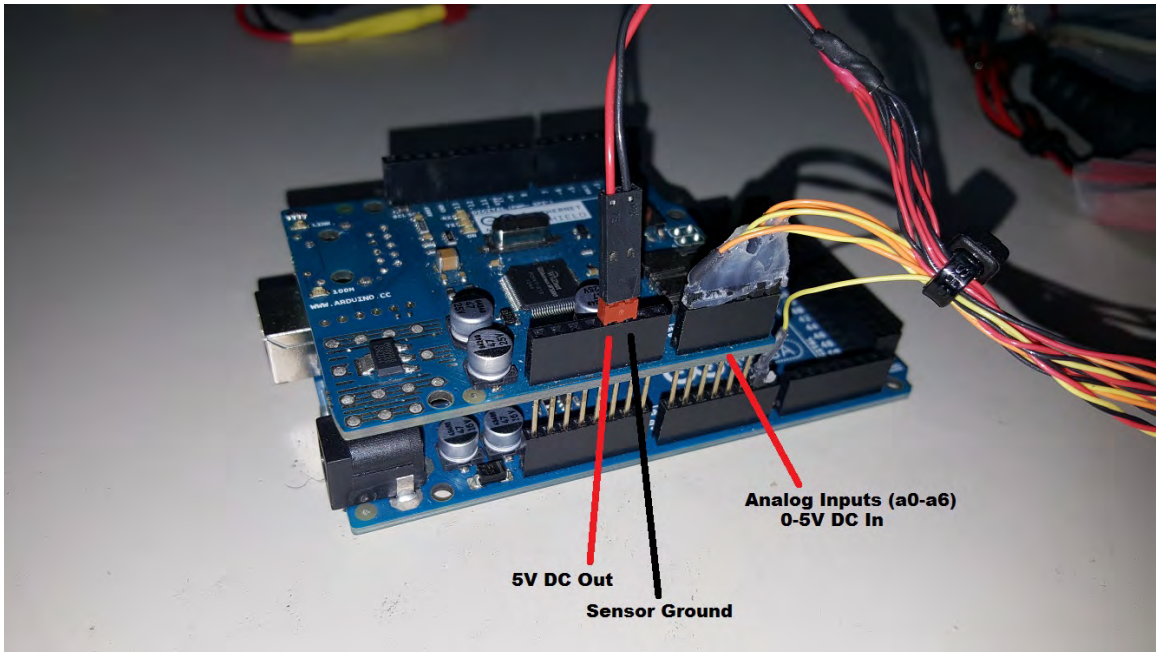

A diagram of the developmental test setup for the Arduino Mega 2650, the Ethernet Shield, and the EEMS is seen below in Figure 15. After we provided power to the Arduino, the Arduino communication terminal was initialized on the laptop and real-time data began appearing on the screen. The log contained eight columns of data. The first seven columns contained seemingly arbitrary numbers between 0–1024. By inspection, those values equate to a proportion of each analog input's maximum input voltage. For example, a logged value of zero is equivalent to a zero-volt input on that analog input. Likewise, a logged value of 1024 is equivalent to a five-volt input on that input. The increase was found to be proportional and completely linear.

Figure 15. Developmental test configuration for Arduino Mega with Ethernet Shield

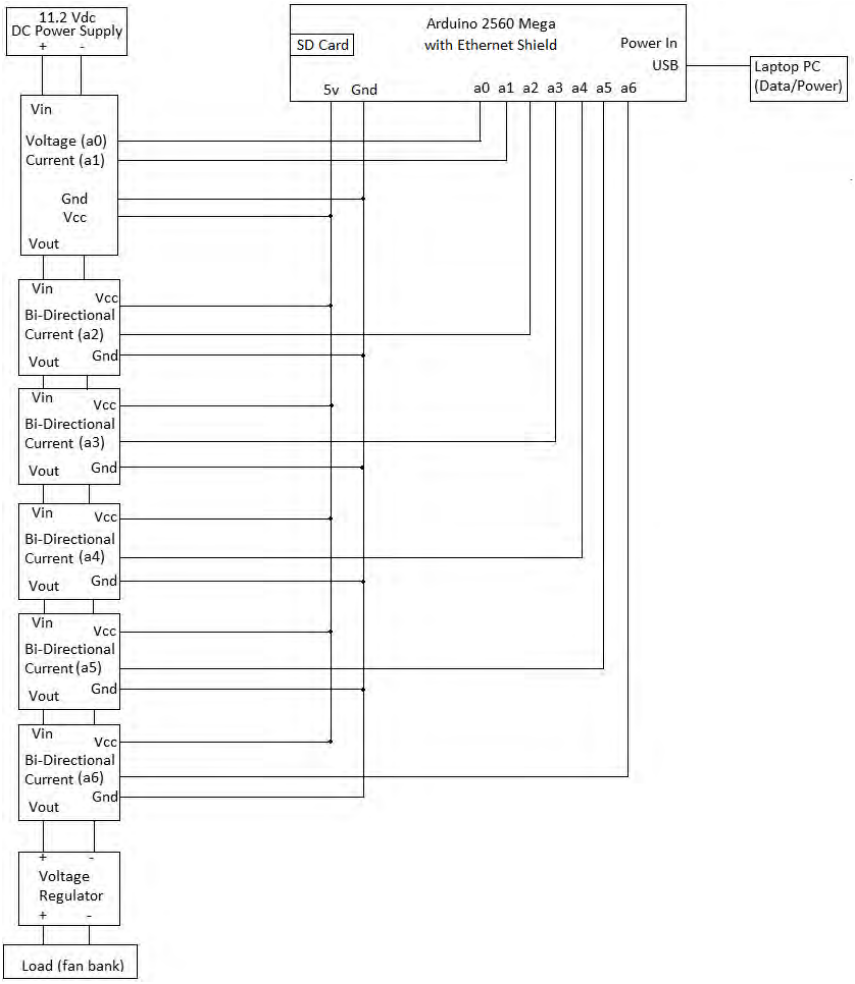

This information becomes important when looking at the bi-directional current sensors installed on inputs a2 through a6. These sensors are bi-directional, and their outputs are voltages between 0 and 5 V_{DC}, depending on the current at that sensor. Each of these sensors' outputs were required to be scaled. Likewise, each sensor has a different zero point which must be determined based on the onboard potentiometers. This was accomplished through inputting known currents into the sensors and conducting a regression analysis on the output values prior to obtaining any operational testing results. Examples are shown in Table 1, as well as Figure 16 in a graphical form.

Table 1. Analog inputs with corresponding coefficients and zero point values

Input	Scaling Coefficient	Scaling Stand. Error	Y-Intercept	Y-Intercept Stand. Error
a2	150	<.01%	836	<.01%
a3	159	3%	837	<.01%
a4	142	2%	856	<.01%
a5	136	1.7%	841	<.01%
a6	165	1.5%	50	2%

Analog inputs a3, a4, and a5 receive signals from the sensors that will detect the current flowing into and out of the batteries during the operational test. It is important that the maximum amount of current being sent into each battery, which we anticipate to approach one ampere, be readable by the sensors. Normally, this is done by adjusting the potentiometers on each sensor. By inspection, Camacho completed this work when he developed the EEMS harness. The maximum current level readable by these sensors ranges between 1.2A and 1.4A each.

Figure 16. Determination of zero point and scaling coefficients for each sensor

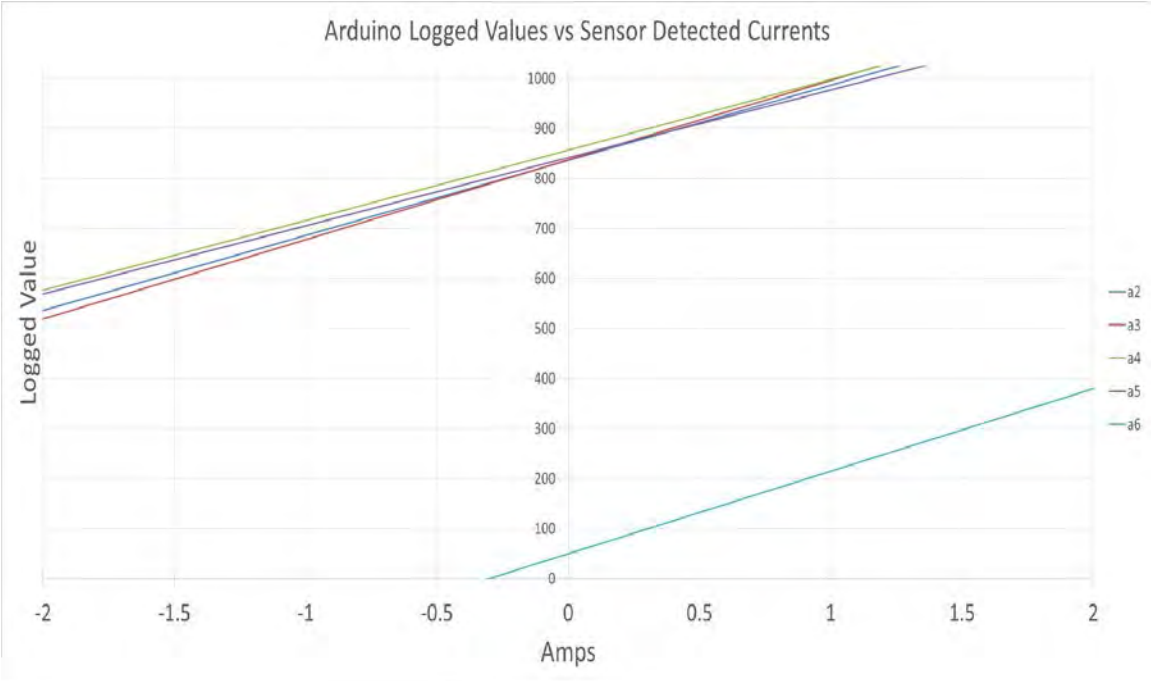

D. OPERATIONAL TESTING RESULTS

With regard to the systems engineering "vee" model, the commencement of operational testing is typically located at the lower-to-middle of the right side of the "vee," with the next step being verification and validation. The operational test of the power management system was conducted from September 14–21 2015. The test began at 1530L and was left in operation for nearly a complete week on the roof of Spanagel Hall, at the Naval Postgraduate School in Monterey, CA. The environmental conditions varied throughout the week, with the first two days of the test experiencing fairly heavy fog, and generally cloud covered periods of daylight. During the final four days of the test, improved solar conditions were noted throughout.

1. Test Rig Setup

Protection from environmental conditions had to be planned for in this test. As such, the entire system with the exception of the wing-mounted array was installed into a weather-resistant plastic container. All electrical leads into and out of the enclosure were

routed through grommets in the sides of the container. These grommets provided penetration points in the container while maintaining its weather-resistance.

It was important to keep the entire test rig stationary but most importantly the wings. As such, the wings were placed onto a sheet of insulating foam for protection from abrasions with the floor, and secured with elastic straps, as shown in Figure 17 below. The straps were located as not to interfere with the irradiance of the PV cells. The foam board was secured to the floor with those same straps, a series of aluminum angle brackets, and with various weights to anchor the system in case of high winds.

Figure 17. Wing mounted array secured to a foam backing board during the operational test

Internal to the enclosure, foam was closely fitted around each of the components, to include the load and its regulator. Functionally, this kept the load operating as consistently as possible; without this foam, it was likely that the wiring could have

hindered the fans' operation by being caught in the blades. The enclosure and its components are shown in Figure 18.

Figure 18. Operational test enclosure setup

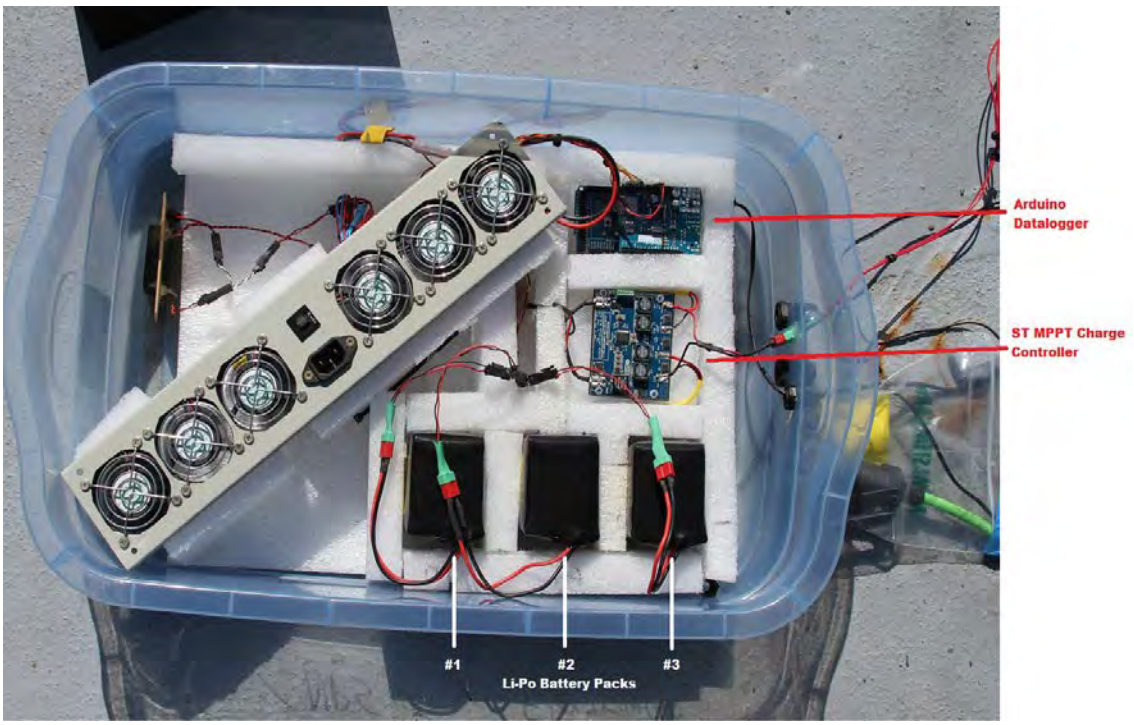

With regard to the Arduino data logging unit, power was provided via a $120V_{AC}$ outlet, so it would not provide an additional load on the system. This was used because leaving a computer unsecured and exposed to environmental conditions was seen as an unreasonable risk solely for the purpose of providing power via a USB port. The EEMS harness was connected to all of the system's components, and its wiring was neatly routed. Upon connection of the 120V power to the Arduino, the test began.

As planned, a transitional state was added into the operational test. Prior to the test, batteries 1 and 3 were placed on a battery testing device and discharged until their voltage levels indicated 15.4 volts. Battery 2 was placed on the same battery testing device and discharged to 14.2 volts. This allowed us to monitor the system's stability in

the case of a battery losing the functionality of a cell. The effect would only be temporary however, as the three parallel battery packs would equalize over the test period.

2. Data Analysis

Over four hundred thousand data samples were collected and stored in a text file according to the Arduino data logging code. The first step in analyzing the data was to import the text file's data samples into MATLAB for processing. Among the questions being considered in the analysis are:

- How much power did the PV cells and MPPT module produce?
- How much power was expected to be produced?
- How much power did the load consume?
- What was the net gain or loss of stored energy?
- Did the system self-regulate the voltage level?
- Did the load ever deplete the batteries to the point of a system shutdown?
- Where is the constraint in the system?

a. Total Energy Produced

The total amount of energy produced by the combination of the PV panel and the MPPT module during the test can be determined using equation 3.

$$Total\ Energy\ (Watt - Days) = \int_{TimeDays=0}^{TimeDays=7} a_0 voltage * a_2 current \qquad (3)$$

Where $a_0$voltage represents the logged analog DC voltage (in volts) present on the EEMS bus, and $a_2$current represents the logged analog current (in amps) to all components as represented in Figure 19. The components with bold borders denote the changes in the configuration from the developmental tests.

Figure 19. Operational testing configuration

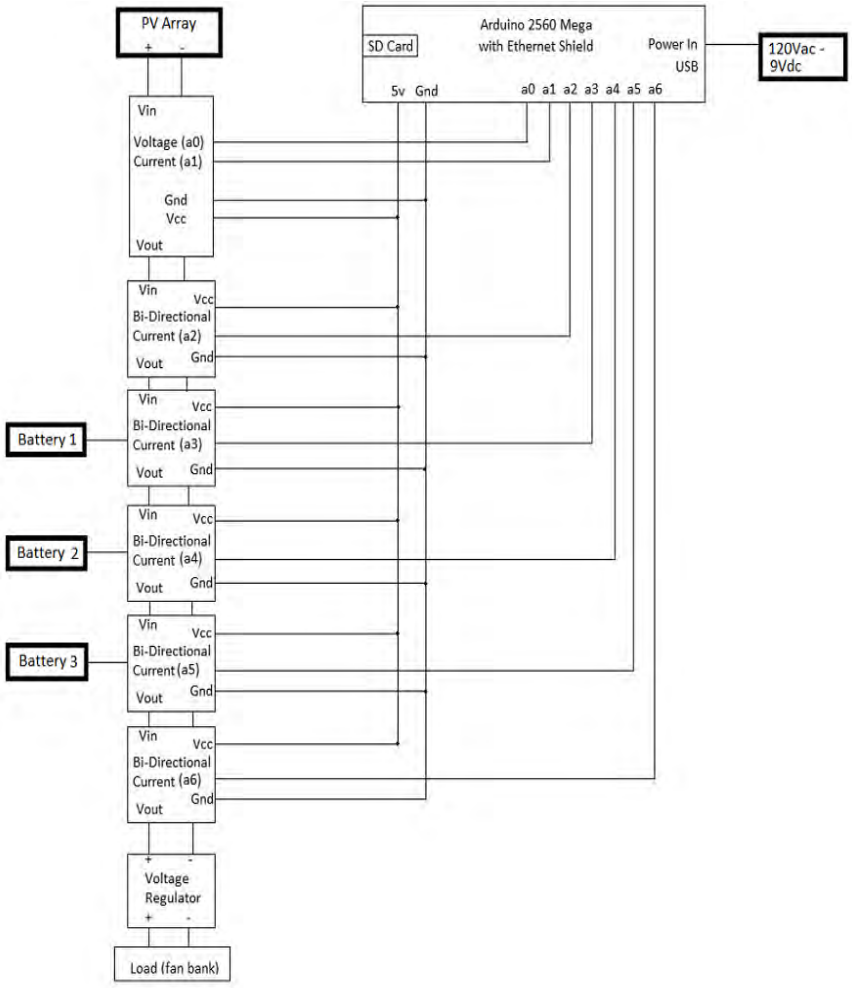

When using MATLAB as the analysis tool, this operation was accomplished by the “trapz” function. This function is used to estimate the integral value using a provided set of x-y pairs in the absence of an actual function that can be evaluated. Figure 19 shows the MPPT output, which is represented by the blue line, over the seven-day testing period.

Figure 20. Power output from MPPT during operational test

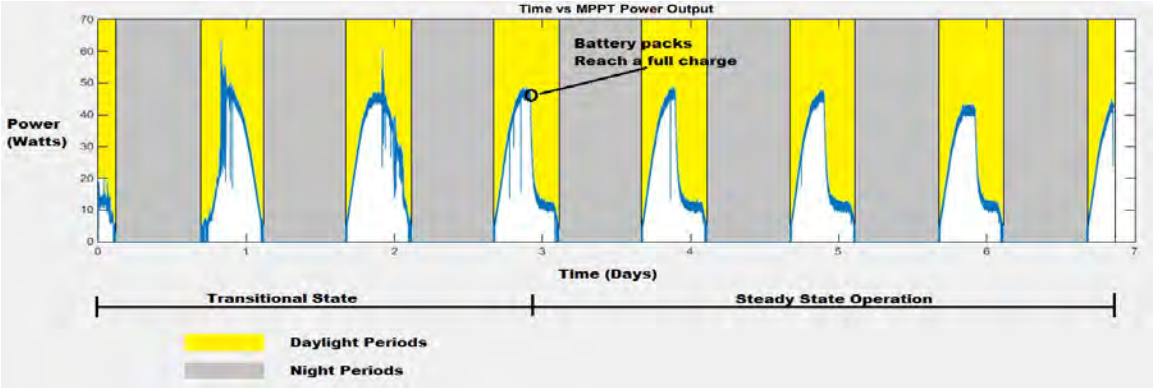

The total amount of energy produced over the operational testing period was determined via MATLAB to amount to 71.1178 watt-days, or 1706.82 watt-hours. This value is important to find because the energy must be accounted for as it is used or stored by the system's various components. This helped to determine any losses in the system.

Two states are clearly shown in Figure 20: the transitional state, which occurs during the first three days of the test, and the steady state, which begins in the middle of day three and continues until the end of the test. The transitional state was purposely induced to determine whether the system could actually transition out of it. In real-life conditions, this transitional state would occur if TaLEUAS were to operate in an area which received little direct sunlight on its PV array for an extended period.

In the steady state, which is considered the system's normal operating mode, the MPPT begins producing power at the instant the MPPT's input voltage crosses the $6.5V_{DC}$ threshold. This power output increases until the solar irradiance level peaks (whether by cloud cover, or transition to night time), or the battery packs reach a full charge, indicated by a bus voltage of $16.68V_{DC}$. This dramatic drop in output power was seen daily, and noted in Figure 20.

b. Total Energy Expected

The total amount of energy expected is based on several factors. The first is solar irradiance level, which varies based on latitude, time of year, and environmental

conditions such as fog or sky cover. The National Renewable Energy Laboratory (NREL) provides public access to a wealth of knowledge pertaining to local expected irradiance levels. By entering the location and date of the test, NREL projects the hourly amount of energy that will be projected onto a square meter of PV cells, based on historical data. Using this information, along with the actual area of the PV array and advertised cell efficiency, the expected MPPT output power can be determined. This is shown in Equation 4.

$$MPPTPowerExpected = Array\ Irradiance * Array\ Area * \eta_{pv} * \eta_{mppt} \quad (4)$$

The MPPT power expected is expressed in watts, the array irradiance is expressed in watts per square meter, and the array area is expressed in square meters. The PV cell and MPPT efficiencies are unit-less ratios. The power can then be integrated over time to give energy. The energy expected was calculated and plotted against the actual energy produced to help find any anomalies. An example is shown in Figure 21.

Figure 21. Comparison of actual MPPT power output values with historical data (values obtained from NREL PVWatts Calculator)

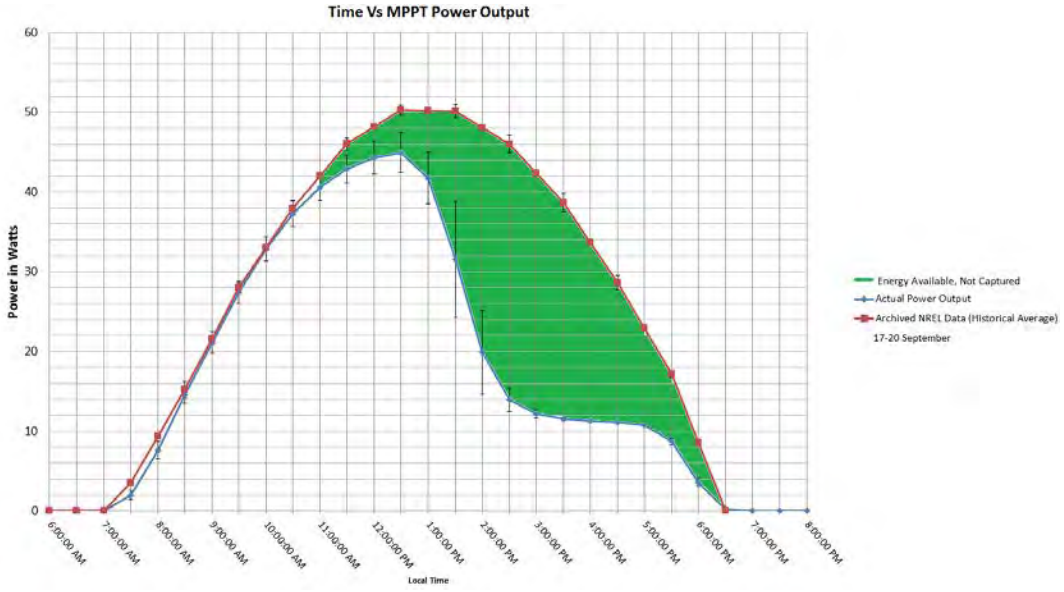

The red line represents the expected MPPT output based on the location of the test and date, using PV array irradiance values provided by NREL, the measured PV array area, and efficiencies as advertised. The blue line shows the actual MPPT output power from the 17th through the 20th of September. These bi-hourly power figures were obtained by first affecting a moving average of every 30 minutes' worth of individual sensor readings. Next, those moving averages for each 30 minute segment were averaged across the same times each day for the four day period. Lastly, the standard-error across the 4 averages was calculated, and is shown in the error bars on the plot. A similar process was followed using NREL's historical data.

There is an easily noticeable offset between the blue and red lines, which may be at least partly accounted for by different conditions on the days when the archived data was recorded. The power output peaked almost as expected; however, immediately after the peak, the power output dropped dramatically. Again, this was due to the battery packs reaching a state of full charge, and was expected.

Another important aspect shown in Figure 21 is the area shown in green. This area represents the amount of PV energy that was available but ultimately not captured electrically. This is due to the maximum voltage being detected on the EEMS bus which indicates full batteries. This occurred daily while operating in a steady state. Therefore, we can express that either a shortage of energy storage, an excess capacity for charging, or the ability to power a larger load exists. Given the mission of TaLEUAS, and the reliance on PV-produced-energy to survive through the night, the former is the likely better expression of the three. The expected amount of energy over the nearly seven- day period based on the NREL prediction was 88.51 watt-days or 2124 watt-hours.

c. Load Energy Consumption

The load, which was provided by the bank of six small fans, consumed the vast majority of all of the energy produced. A $12V_{DC}$ voltage regulator was placed before the fan bank, and according to each fan's specification for current draw (.13A), the fan bank nominally required 9.36 watts of power. A plot of the power consumed over the operational testing period is shown below in Figure 22.

Figure 22. Power consumption of the load during operational testing.

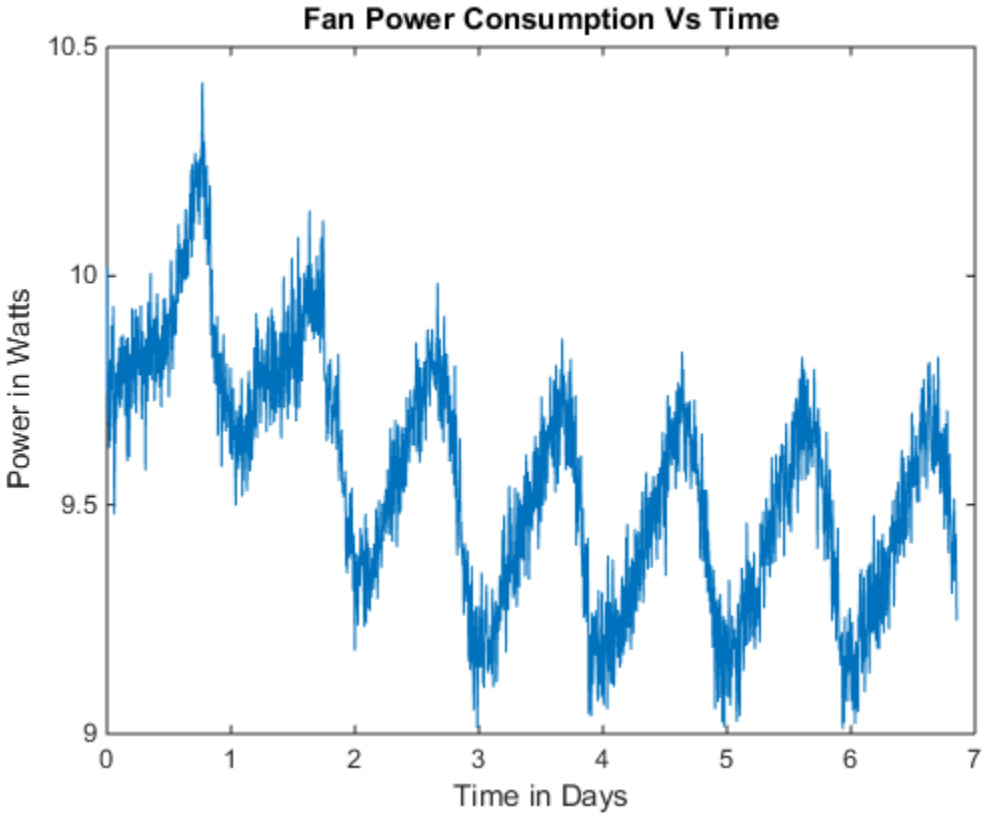

The blue line represents the power consumed in watts, as calculated using the voltage regulator's $12V_{DC}$ output voltage, and the logged current values throughout the testing period. The voltage regulator is roughly 90 percent efficient, but this loss was accounted for due to the current sensor's "upstream" installation. Once again, the "trapz" function was used in MATLAB to determine the total energy consumed, and was ultimately calculated to be 65.51 watt-days, or 1572.24 watt-hours. The cyclical display of the power output can be explained by either voltage or current fluctuations throughout the day. The majority of the wattage readings are within a half-watt from the mean, so this was not a concern. Figure 22 also shows another important fact; the load was never dropped overnight. Energy was continuously consumed.

At this point, it has been shown that the amount of energy produced by the PV array and MPPT has exceeded what has been consumed by the load. Therefore, the remaining energy must either be lost to heat, or is stored in the battery packs.

d. Net Gain or Loss of Energy

The net gain or loss of energy can be determined in the same way as the previous calculations. However, with the amount of energy produced and consumed already calculated, the safe assumption is that a net gain occurred and is stored in the battery packs. This is partly due to the interpretation of the bus voltage plot and its positive sloping trend, seen in Figure 23 below.

Figure 23. EEMS bus voltage over the operational testing period.

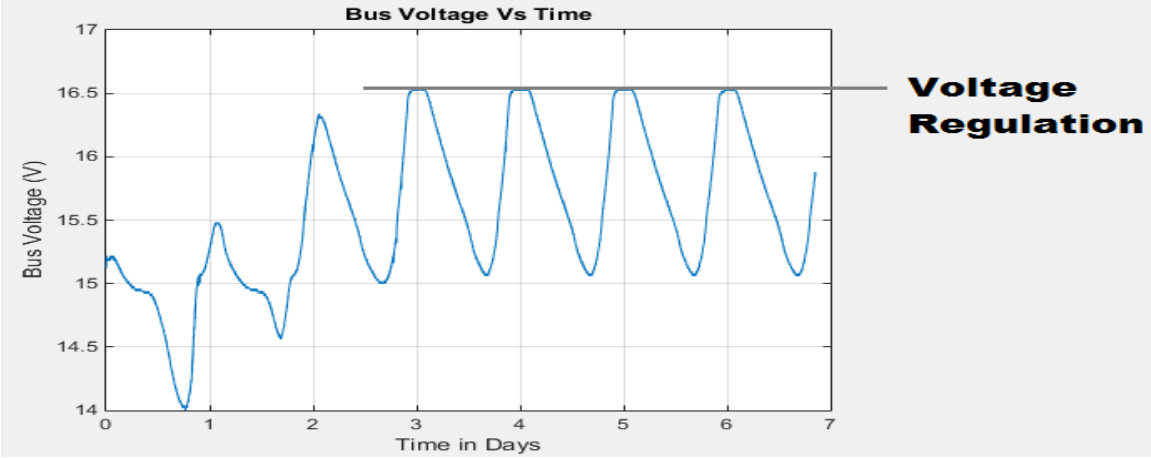

Figure 23 also shows that the intended voltage regulation is occurring in the clipped upper portions of the waveform, as seen from day 3 until completion.

Each pack had its own bi-directional current sensor installed. This allowed the tracking of power both into and out of each battery during the day and at night. The plot of the three battery packs is shown in Figure 24.

Figure 24. Daily power input and output to/from the battery packs during operational testing.

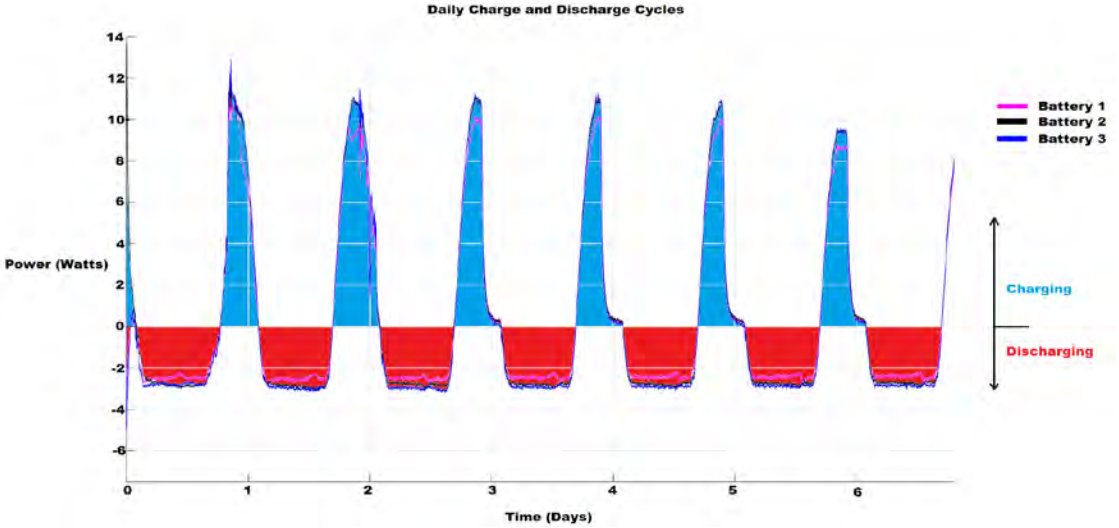

Figure 24 shows the power both stored in and taken from each battery, over the entire testing period. The blue areas represent periods where the batteries are in a charging state, and red areas represent a discharging state. In the initial hour of the test, the abbreviated transitional period can be seen. Battery 2 is the only pack which is charging while the other two are in a state of discharge. This is not only due to providing power to operate the load, but batteries 1 and 3 are also charging battery 2, as intended. Figure 24 shows an enhanced view of the pack voltages over a single day during the steady state period.

Figure 25. Steady state operation of battery packs

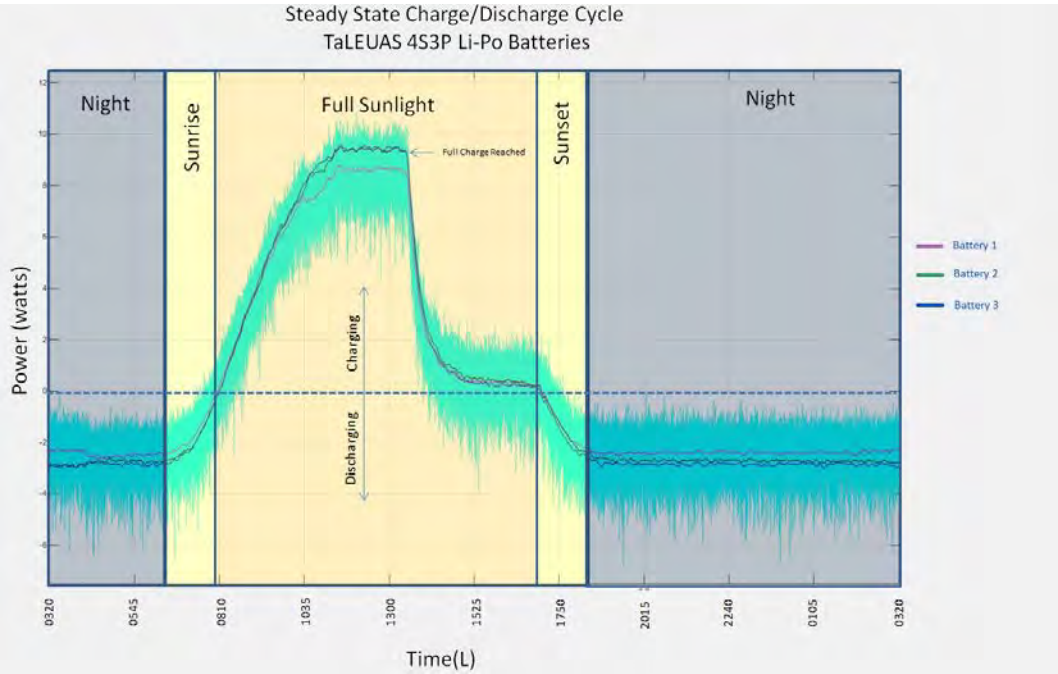

The cyan colored line in Figure 25 shows the actual sensor reading from analog pin 3, which read the current into and out of battery 1. The other battery current sensors were similar, and required processing. A smoothing function was implemented on the data imported from sensors a3, a4, and a5 to run a moving average for every five minutes of data, and is shown in the magenta, green, and blue lines.

Ultimately, MATLAB's "trapz" function again provided the integrated values for the power stored and expended in each battery over the testing period. All three batteries showed net gains to the energy stored. See Table 2.

Table 2. Gains and losses for each battery pack during operational testing.

	Energy In	Energy Out	Net	Units
Battery 1	12.16	10.13	2.03	
Battery 2	13.44	11.3	2.14	
Battery 3	13.24	11.94	1.3	
Total	38.84	33.37	**5.47**	watt-days

V. CONCLUSION

The completion of this phase of the study leads to a number of important conclusions which help to bridge the capability gap that this research sought to address. The primary results show that the current configuration of the power management system is suitable for continuously powering a 10 watt load. There is ample power generation from current solar cell technology to support continuous UAS flight. However, there are significant shortfalls in battery capacity that prevent the full use of collected solar energy. The mixture of test results suggests that further research and development has great potential to improve the viability of TaLEUAS's overnight longevity.

Our main objectives in this study were to design, build, and test a power interface for use aboard TaLEUAS. By using the systems engineering process, we derived stakeholder and system requirements, which placed constraints on possible solutions. In turn, these requirements became the main driver for potential system designs. Through a series of experiments and review of past efforts, a subset of alternatives was developed for testing. What emerged was a fully-autonomous power system with the capability to continuously operate a reduced load and charge li-po batteries safely. Although this breakthrough furthered the technology necessary to support persistent ISR, it also uncovered challenges that include an inability to power the UAS when it is outfitted with its full complement of subsystems. Foremost in these issues is that the addition of a propulsion motor will require further research and development in battery technology.

A. ASSESSMENTS

The following assessments were reached upon completion of the operational test:

- The power management system, in its current state, is fully suitable for continuously operating a load of approximately 10 watts, autonomously. This is significant because the avionics suite planned for installation in the next generation TaLEUAS consumes approximately this amount of power. However, the avionics subsystems do not operate in isolation aboard the craft, thus creating a new power demand.

- The power management system is not suitable for operating any future avionics suites in combination with the installed propulsion system. It is a problem that results from insufficient onboard energy storage capacity. Though the system is capable of operating the avionics suite overnight without interruption (even with a safety margin), the propulsion motor operating simultaneously will consume enough energy to quickly deplete the batteries. Regardless of any future improvements in power management, the capacity of the battery packs will limit the utility of the entire power system.

- The primary constraint in the entire power system remains the battery packs, specifically their energy densities. The difficulty in significantly increasing the energy density locally through battery modification has a direct impact on efforts being devoted to reduce the weight of the aircraft structure and other components. A full system model for TaLEUAS that determines the effects of changes to individual component performance and/or size can help estimate a design point that may be able to reliably achieve continuous flight.

- There is great potential to explore experimentation and optimization methods to develop new design configurations. From a total-system perspective, a series of energy equations can be used to describe the behavior of the system. Equation 5 is a high-level constraint which may rarely be violated, and only on a day with a low amount of solar radiance in combination with an oversized battery bank. This is because in practice, the batteries fall outside of the energy balance since they aren't true sources or sinks for energy; only storage. Equations 6 and 7 expand on this.

$$E_{in} \geq E_{out} \tag{5}$$

$$E_{in} = E_{solar} + E_{thermal} \tag{6}$$

$$E_{out} = E_{avionics} + E_{propulsion} \tag{7}$$

E_{in} represents the total amount of energy from both solar (E_{solar}) and thermal ($E_{thermal}$) sources. E_{out} represents the total amount of energy expended by the onboard avionics ($E_{avionics}$) and propulsion ($E_{propulsion}$) systems.

Expanded upon further, Equations 8 and 9 are used to calculate the total amount of solar and thermal energies harvested, respectively. Equations 10 and 11 calculate the energy expended in the avionics and propulsion systems, respectively.

$$E_{solar} = A * \eta_{pv} * R * cos(\theta) \quad (8)$$

$$E_{thermal} = \Delta h * m * g \quad (9)$$

In the determination of the amount of solar energy harvested by the solar array, A represents the area of the array. The efficiency of the PV array is represented by η_{pv}. R represents the solar irradiance, and θ represents the angle between the array and the sun. Equation 9 is a measure of potential energy gained by soaring, where Δh represents the change in altitude, m represents the mass of the aircraft, and g represents acceleration due to Earth's gravity.

$$E_{avionics} = \sum(P_{comp} * T_{comp} * \eta_{comp}) \quad (10)$$

$$E_{propulsion} = \sum P_{propulsion} * T_{propulsion} * \eta_{motor} * \eta_{esc} * \eta_{propeller} \quad (11)$$

When quantifying the total amount of energy expended in the operation of the avionics system ($E_{avionics}$), P_{comp} represents the power required to operate a component. T_{comp} represents the time that component was in use, and η_{comp} represents the efficiency in the voltage converting components. The summation allows for a variety of components with different power levels and run times. In Equation 11, $P_{propulsion}$ represents the electrical power delivered to the propulsion system; $T_{propulsion}$ represents the amount of time that the propulsion system is operated. The efficiencies of the motor, electronic speed control, and propeller are represented by η_{motor}, η_{esc}, and $\eta_{propeller}$, respectively.

With regard to the battery packs, Equation 12 can be used to quantify the total amount of energy stored in them.

$$E_{batt} = m_{batt} * E_{sp} * \eta_{batt}. \quad (12)$$

In Equation 12, m_{batt} represents the mass of the battery. E_{sp} represents energy density. Lastly, η_{batt} represents a practical efficiency due to the inability to drain the battery entirely without damaging or destroying it. This is required because certain battery chemistries can be damaged from over-discharge. The li-po packs in use in our

case need to maintain a charge of at least fifteen percent; discharge beyond that significantly shortens the longevity of the battery.

Working through an example problem leads us to the determinations for required battery weight, as well as required PV array size. Assumptions are made that the propulsion system is unused, and that the avionics load is a constant 9 watt draw with no losses.

$$T_{propulsion} = 0$$

$$E_{avionics} = (9W) * (24\ hours) * (1) = 216\ Wh$$

Assuming 16 hours of darkness, or insufficient irradiance to energize the avionics, the energy drawn from the battery is calculated as:

$$E_{batt} = (9W) * (16\ hours) = 144\ Wh$$

When substituted into Equation 12, with the known E_{sp} value, and our stated η_{batt} of 85%, the mass of the battery required to operate the load is calculated as:

$$m_{batt} = \frac{E_{batt}}{E_{sp} * \eta_{batt}} = \frac{144\ Wh}{170\frac{Wh}{Kg} * .85} = 1kg\ minimum$$

Lastly, rearranging Equation 8 can aide in the determination of the necessary PV array size.

$$A = \frac{E_{solar}}{\eta_{pv} * R * cos(\theta)} = \frac{216\ Wh}{(.225) * (5.08\frac{kWh}{m^2})} = .2\ m^2\ minimum$$

B. FUTURE RESEARCH

An optimization problem exists when considering the onboard energy storage capacity, the charging capacity, and the load. Given that each battery pack weighs 521 grams and provides 88.8 watt-hours of energy (only about 71 watt-hours can be used without degradation to the battery longevity), this translates into a specific energy of 136 watt-hours/Kg. This tradeoff is simple in that every watt-hour of usable energy "weighs" 7.33

grams. This is likely already the best available choice with regard to energy density, and through modelling and trade space analysis this can be verified. However, there is a point where energy storage, and thus weight, becomes excessive.

Given a 9 watt load, over a 16 hour period of darkness, the load would consume 144 watt-hours of energy. This equates to 1055 grams of required energy storage capacity when li-po batteries are used. Likewise, given that three battery packs were used during the operational test, the 1563 grams of capacity is enough to fully support the load and provide a small bit of a safety factor. Further improvement in the battery's energy density would provide the greatest benefit in weight reduction for the power system.

Modify the MPPT circuit architecture or PV array configuration to enable the installation of multiple MPPT modules that will provide redundancy and overall efficiency. The charging capacity is dictated by the MPPT module and the PV array. It is currently hampered by the ISV009v1's requirement for a minimum operating voltage of 6.5 volts. Lowering this minimum operating voltage enables the harvesting of solar energy at lower radiance levels, primarily at sunrise and sunset.

Lastly, reduce the propulsion system's power requirement through further lightening of the airframe (specific energy improvement) to further enable TaLEUAS to autonomously glide in a truly continuous fashion. The propulsion system's power requirement, and the airframe's weight are truly the determining factors in how many TaLEUAS craft are required to complete a given intelligence, surveillance, and reconnaissance (ISR) mission.

THIS PAGE INTENTIONALLY LEFT BLANK

APPENDIX A. ARDUINO DATALOGGING CODE

```
/*
  SD card datalogger

This example shows how to log data from three analog sensors
to an SD card using the SD library.

The circuit:
* analog sensors on analog ins 0, 1, and 2
* SD card attached to SPI bus as follows:
** MOSI - pin 11
** MISO - pin 12
** CLK - pin 13
** CS - pin 4

created  24 Nov 2010
modified 9 Apr 2012
by Tom Igoe – modified by V. Dobrokodov and R. Fauci

This example code is in the public domain.

*/

#include <SPI.h>
#include <SD.h>

const int chipSelect = 4;

void setup()
{
  // Open serial communications and wait for port to open:
  Serial.begin(9600);
  while (!Serial) {
    ; // wait for serial port to connect. Needed for Leonardo only

  }


  Serial.print("Initializing SD card...");

  // see if the card is present and can be initialized:
  if (!SD.begin(chipSelect)) {
    Serial.println("Card failed, or not present");
```

```
    // don't do anything more:
    return;
  }
  Serial.println("card initialized.");
}

void loop()
{

  // make a string for assembling the data to log:
  String dataString = "";

  // read seven sensors and append to the string:
  for (int analogPin = 0; analogPin < 7; analogPin++) {
    int sensor = analogRead(analogPin);

    dataString += String(sensor) ;
    if (analogPin <= 6) {
      dataString += ,"";
      delay(175);
    }
  }
  // form and append a timestamp
  dataString+=String(millis()/1000.,DEC);
  // open the file. note that only one file can be open at a time,
  // so you have to close this one before opening another.
  File dataFile = SD.open("datalog.txt," FILE_WRITE);

  // if the file is available, write to it:
  if (dataFile) {
    dataFile.println(dataString);
    dataFile.close();
    // print to the serial port too:
    Serial.println(dataString);
  }
  // if the file isn't open, pop up an error:
  else {
    Serial.println("error opening datalog.txt");
            }
```

APPENDIX B. MATLAB PROCESSING CODE

```
%----------Determining MPPT Power Output----------------
MPPTPower=a1BusVoltage.*a2BusBDC;
MPPTPowerRefPos=MPPTPower>=0;

MPPTPowerMultPos=MPPTPower.*MPPTPowerRefPos;


time=transpose(TimeDays);

vel=transpose(MPPTPowerMultPos);

figure(1)
plot(TimeDays,MPPTPower)
title('Time vs MPPT Power Output');


MPPTPowerTotal = trapz(time,vel) %Power in Watt-Days
%-------------------------------------------------------

%----------Determining Power Into Battery 1--------------
Bat1Power=a1BusVoltage.*a3Bat1BDC;
Bat1PowerRefPos=Bat1Power>=0;
Bat1PowerRefNeg=Bat1Power<=0;
Bat1PowerMultPos=Bat1Power.*Bat1PowerRefPos;
Bat1PowerMultNeg=Bat1Power.*Bat1PowerRefNeg;

vel1=transpose(Bat1PowerMultPos);
vel11=transpose(Bat1PowerMultNeg);

figure(2)
subplot(1,2,1), plot(TimeDays,Bat1Power)
subplot(2,2,2), plot(TimeDays,Bat1PowerMultPos)
subplot(2,2,4), plot(TimeDays,Bat1PowerMultNeg)

Bat1PowerIn = trapz(time,vel1) %Power in Watt-Days
Bat1PowerOut = trapz(time,vel11)
Bat1PowerNet = Bat1PowerIn-abs(Bat1PowerOut)
%-------------------------------------------------------

%----------Determining Power Into Battery 2--------------
Bat2Power=a1BusVoltage.*a4Bat2BDC;
Bat2PowerRefPos=Bat2Power>=0;
```

```
Bat2PowerRefNeg=Bat2Power<=0;
Bat2PowerMultPos=Bat2Power.*Bat2PowerRefPos;
Bat2PowerMultNeg=Bat2Power.*Bat2PowerRefNeg;

vel2=transpose(Bat2PowerMultPos);
vel22=transpose(Bat2PowerMultNeg);

figure(3)
subplot(1,2,1), plot(TimeDays,Bat2Power)
subplot(2,2,2), plot(TimeDays,Bat2PowerMultPos)
subplot(2,2,4), plot(TimeDays,Bat2PowerMultNeg)

Bat2PowerIn = trapz(time,vel2) %Power in Watt-Days
Bat2PowerOut = trapz(time,vel22)
Bat2PowerNet = Bat2PowerIn-abs(Bat2PowerOut)
%----------Determining Power Into Battery 3----------

Bat3Power=a1BusVoltage.*a5Bat3BDC;
Bat3PowerRefPos=Bat3Power>=0;
Bat3PowerRefNeg=Bat3Power<=0;
Bat3PowerMultPos=Bat3Power.*Bat3PowerRefPos;
Bat3PowerMultNeg=Bat3Power.*Bat3PowerRefNeg;

vel3=transpose(Bat3PowerMultPos);
vel33=transpose(Bat3PowerMultNeg);

figure(4)
subplot(1,2,1), plot(TimeDays,Bat3Power)
subplot(2,2,2), plot(TimeDays,Bat3PowerMultPos)
subplot(2,2,4), plot(TimeDays,Bat3PowerMultNeg)

Bat3PowerIn = trapz(time,vel3) %Power in Watt-Days
Bat3PowerOut = trapz(time,vel33)
Bat3PowerNet = Bat3PowerIn-abs(Bat3PowerOut)
%-------------------------------------------------------
BatPowerInTotal=Bat1PowerIn+Bat2PowerIn+Bat3PowerIn
BatPowerOutTotal=Bat1PowerOut+Bat2PowerOut+Bat3PowerOut
BatPowerNet=Bat1PowerNet+Bat2PowerNet+Bat3PowerNet
%----------The Battery Plot----------------------------
figure(8)
plot(TimeDays,Bat1Power,'c')
hold
plot(TimeDays,bat1,'m')
plot(TimeDays,bat2,'k')
plot(TimeDays,bat3,'b')
```

```
axis([5.5 6.5 -7.5 12.5]);
grid on;

%----------Determining Power Into Fan Load----------------
FanPowerConsumed=12*a6smooth;

vel4=transpose(FanPowerConsumed);

figure(5)
plot(TimeDays,FanPowerConsumed)

FanPowerConsumed = trapz(time,vel4) %Power in Watt-Days
%
Losses=MPPTPowerTotal-abs(BatPowerNet)-FanPowerConsumed

figure(6)
plot(TimeDays,a1BusVoltage)
```

THIS PAGE INTENTIONALLY LEFT BLANK

LIST OF REFERENCES

Arduino. 2015. “Arduino Mega 2560 Overview.” Accessed August 24. https://www.arduino.cc/en/Main/ArduinoBoardMega2560.

Camacho, Nahum. 2014. “Improving Operational Effectiveness of Tactical Long Endurance Unmanned Aerial Systems (TALEUAS) by Utilizing Solar Power.” Master’s thesis, Naval Postgraduate School.

Eagle Tree Systems. 2013. “Elogger v4.” Accessed July 2, 2015. http://www.eagletreesystems.com/index.php?route=product/product&path=62&product_id=54.

———. 2015. *Instruction Manual for the eLogger V4.* Bellevue, WA: Eagle Tree Systems. http://www.eagletreesystems.com/Manuals/eLogger%20V4%20Instruction%20Manual.pdf.

Ragonese, D. and Ragusa, M. 2012. “AN3392 Application Note - Designing with the SPV1020, an Interleaved Boost Controller with MPPT Algorithm.” Accessed September 23. http://www.st.com/st-web-ui/static/active/en/resource/technical/document/application_note/DM00026751.pdf.

Stephenson, Christopher. 2012. “Utilizing Maximum Power Point Trackers in Parallel to Maximize the Power Output of a Solar (Photovoltaic) Array.” Master’s thesis, Naval Postgraduate School.

Stevens, Roger. 1979. Operational Test & Evaluation: *A Systems Engineering Process*. Malabar, FL: Robert E. Krieger.

STMicroelectronics. 2011. “STEVAL-ISV009V1 - 300W Photovoltaic Converter Demonstration Board Based on the SPV1020 - Data Brief.” Accessed September 23. http://www.st.com/web/en/catalog/tools/PF251965.

THIS PAGE INTENTIONALLY LEFT BLANK

INITIAL DISTRIBUTION LIST

1. Defense Technical Information Center
   Ft. Belvoir, Virginia

2. Dudley Knox Library
   Naval Postgraduate School
   Monterey, California